ACS OMEGA

http://pubs.acs.org/journal/acsodf

Article

Ethyl Acetate Extract of *Colletotrichum gloeosporioides* Promotes Cytotoxicity and Apoptosis in Human Breast Cancer Cells

Nilesh Rai, Priyamvada Gupta, Ashish Verma, Rajan Kumar Tiwari, Prasoon Madhukar, Swapnil C. Kamble, Ajay Kumar, Rajiv Kumar, Santosh Kumar Singh, and Vibhav Gautam*

Cite This: *ACS Omega* 2023, 8, 3768−3784

Read Online

ACCESS | Metrics & More | Article Recommendations | Supporting Information

ABSTRACT: Fungal endophytes are known to be a paragon for producing bioactive compounds with a variety of pharmacological importance. The current study aims to elucidate the molecular alterations induced by the bioactive compounds produced by the fungal endophyte *Colletotrichum gloeosporioides* in the tumor microenvironment of human breast cancer cells. GC/MS analysis of the ethyl acetate (EA) extract of *C. gloeosporioides* revealed the presence of bioactive compounds with anticancer activity. The EA extract of *C. gloeosporioides* exerted potential plasmid DNA protective activity against hydroxyl radicals of Fenton's reagent. The cytotoxic activity further revealed that MDA-MB-231 cells exhibit more sensitivity toward the EA extract of *C. gloeosporioides* as compared to MCF-7 cells, whereas non-toxic to non-cancerous HEK293T cells. Furthermore, the anticancer activity demonstrated by the EA extract of *C. gloeosporioides* was studied by assessing nuclear morphometric analysis and induction of apoptosis in MDA-MB-231 and MCF-7 cells. The EA extract of *C. gloeosporioides* causes the alteration in cellular and nuclear morphologies, chromatin condensation, long-term colony inhibition, and inhibition of cell migration and proliferation ability of MDA-MB-231 and MCF-7 cells. The study also revealed that the EA extract of *C. gloeosporioides* treated cells undergoes apoptosis by increased production of reactive oxygen species and significant deficit in mitochondrial membrane potential. Our study also showed that the EA extract of *C. gloeosporioides* causes upregulation of pro-apoptotic (*BAX*, *PARP*, *CASPASE-8*, and *FADD*), cell cycle arrest (*P21*), and tumor suppressor (*P53*) related genes. Additionally, the downregulation of antiapoptotic genes (*BCL-2* and *SURVIVIN*) and increased Caspase-3 activity suggest the induction of apoptosis in the EA extract of *C. gloeosporioides* treated MDA-MB-231 and MCF-7 cells. Overall, our findings suggest that the bioactive compounds present in the EA extract of *C. gloeosporioides* promotes apoptosis by altering the genes related to the extrinsic as well as the intrinsic pathway. Further in vivo study in breast cancer models is required to validate the *in vitro* observations.

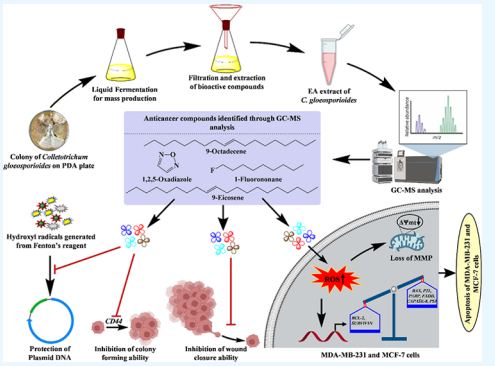

INTRODUCTION

Endophytes are considered as the hidden world inside the host plant organs or tissues. Among endophytic microbial species, fungal endophytes are polyphyletic groups of microorganisms and are known to live asymptomatically in the intracellular or intercellular space of the host tissue, including stems, leaves, and/or roots. In recent years, endophyte research is expanded from cataloging species to studying the characteristics of the endophyte, their interaction with host plants, and the isolation of bioactive compounds of pharmacological significance.[1] The immense biological diversity and the potential ability to produce host-derived bioactive compounds have driven the scientific community to elucidate the pharmacological aspects of fungal endophytes. Various bioactive compounds with potential therapeutic significance including paclitaxel, podophyllotoxin, deoxypodophyllotoxin, camptothecin, hypericin and emodin, azadirachtin, and vinca alkaloids have been identified and characterized from the plant-associated fungal endophytes.[2,3] Numerous hyphenated mass-spectroscopy-based techniques, such as GC/MS, LC/MS, FT-IR, HRMS, and NMR (^{1}H and ^{13}C), are being used to characterize the bioactive compounds produced from fungal endophytes.[4,5] In addition, the bioinformatics tool and *in silico*-based approaches are also being used to study the therapeutic role of natural bioactive compounds produced from either plants or plant-associated microorganisms in many diseases, including cancer.[6−8] Furthermore, fungal endophytes are reported to play a vital role in the maintenance of plant health and growth promotion, which results in an improved potential in plants to acclimatize biotic and abiotic stresses.[9−11] Besides the augmentation of host plant growth and enhancing the

Received: September 5, 2022
Accepted: January 11, 2023
Published: January 20, 2023

resistance of the host plant against biotic and abiotic stress, the fungal endophyte also plays a vital role in the accretion of bioactive compounds similar to their host plants. Fungal endophytes have therefore been demonstrated to produce a wide range of bioactive compounds with potential therapeutic value as well as to protect the host plant species from several pests and infectious diseases.[12,13] Occasionally, the endophytic strains produce novel pharmacologically active and structurally diverse secondary metabolites which are not present in their host's tissues. Thus, it is hypothesized that the endophytes can live independently and produce several bioactive metabolites in association with the host plant.[14] It has been demonstrated that fungal endophyte-derived bioactive compounds are attractive sources of pharmacological leads and can be helpful in the discovery of novel anticancer drugs. In terms of chemical properties, the bioactive metabolites produced by plant-associated fungal endophytes include alkaloids, terpenoids, various polyketides, flavonoids, and other classes of bioactive compounds. Beside these, fungal endophytes are also known as a producer of enzymes including polyketide synthase (PKS) and non-ribosomal peptide synthase. Biosynthetic pathways of many fungal endophyte-derived bioactive compounds include crucial steps which are catalyzed by multifunctional PKS enzymes.[15] A growing body of research has shown that bioactive compounds from well-known fungal genera like *Fusarium*, *Alternaria*, *Curvularia*, *Aspergillus*, *Penicillium*, *Cladosporium*, and *Diaporthe* significantly reduce the risk of cancer, cardiovascular disease, diabetes, and other conditions related to oxidative stress.[16,17] Besides these fungal species, the endophyte *Colletotrichum gloeosporioides* is also reported to be isolated from various plant tissues either in the form of a fungal endophyte or as a plant pathogen.[18] The fungal endophyte *C. gloeosporioides* has been widely explored for the production of bioactive compounds of pharmacological reputation. Various novel bioactive compounds including colletotric acid, ferricrocin, and gloeosporone have been isolated and characterized from the fungal endophyte *C. gloeosporioides* with potential antimicrobial and phytotoxic activities, respectively.[18−20]

The plant *Oroxylum indicum* is a significant source of natural bioactive metabolites with a range of biological activities including anthelmintic, antileucodermatic, antioxidant, anti-bronchitic, and anti-inflammatory activity.[21−23] Considering the host−endophyte interaction, it is hypothesized that the endophyte *C. gloeosporioides* isolated from the leaf tissue of the *O. indicum* plant may also synthesize diverse and unique bioactive compounds of varied pharmacological properties. However, the mechanistic study to elucidate the anticancer activity of the bioactive compounds derived from *C. gloeosporioides* isolated from the leaves of *O. indicum* still remains elusive. Our previous findings have shown that bioactive compounds present in the EA extract of *C. gloeosporioides* show potential antioxidant activity and cytotoxic activity against various human-derived cancer cells.[23] In addition, the EA extract of *C. gloeosporioides* possesses a unique HPTLC fingerprinting profile which may be attributed to antioxidant and cytotoxic activities. Therefore, considering the antioxidant and cytotoxic activities of the bioactive compounds present in the EA extract of *C. gloeosporioides*,[23] the current study aimed to elucidate the molecular mechanism of the anticancer activity of bioactive compound/s produced from *C. gloeosporioides* against breast cancer. The anticancer mechanism of the EA extract of *C. gloeosporioides* was demonstrated through DAPI staining, colony formation assay, and alteration in the expression of genes and proteins. The morphological changes observed in the nucleus of human breast cancer cells treated with the EA extract of *C. gloeosporioides* indicate the onset of apoptosis. The EA extract of *C. gloeosporioides* also substantially inhibited the long-term colony-forming ability and wound closure efficiency of breast cancer cells. We also observed the increased production of reactive oxygen species (ROS) and significant deficits in mitochondrial membrane potential (MMP) in MDA-MB-231 and MCF-7 cells treated with the EA extract of *C. gloeosporioides*. The putative mechanism by which the EA extract of *C. gloeosporioides* potentiates antiproliferation and apoptosis is shown by enhanced Caspase-3 activity and altered expression of genes and proteins related to apoptosis in MDA-MB-231 and MCF-7 cells. Further, the current study will be significantly helpful in the isolation and characterization of novel natural anticancer compounds for the treatment of breast cancer.

MATERIALS AND METHODS

Fermentation and Extraction of the Fungal Endophyte *C. gloeosporioides*. The fungal endophyte *C. gloeosporioides* (accession number LC585212) used in the current study was isolated and identified in our previous study from the healthy leaf tissue of *O. indicum* plant using the culture-dependent approach.[23] Liquid fermentation of the fungal endophyte *C. gloeosporioides* was carried out in an Erlenmeyer flask containing 300 mL of potato-dextrose broth added with 250 μg/mL streptomycin. The flasks were placed in an orbital shaker incubator at 27 ± 2 °C for 21−24 days at 120 rpm. Post-fermentation, the grown mycelium of *C. gloeosporioides* was filtered through a double-layered cheesecloth and was dried at 50 °C for 24 h. Dried mycelium was subjected to liquid nitrogen, followed by maceration. The organic solvent ethyl acetate (EA, 5× volume) was used for the extraction of crude fungal extract. The organic phase containing bioactive compounds produced by the fungal endophyte *C. gloeosporioides* was separated and evaporated to dryness using a rotary evaporator at 30 °C.[24] The resulting fungal extract was weighed and stored at 4 °C for subsequent experiments.

Characterization of the EA Extract of *C. gloeosporioides* Using Gas Chromatography−Mass Spectrometry Analysis. Gas chromatography−mass spectrometry (GC/MS) analysis was carried out to evaluate the presence of volatile organic compounds present in the EA extract of *C. gloeosporioides* with potential antioxidant and anticancer activities. The EA extract of the fungal strain *C. gloeosporioides* was prepared and subjected to a gas chromatograph (Thermo Trace 1300 GC) coupled with a mass spectrometer (MS Thermo TSQ 8000). For, GC/MS analysis, approximately 99.9% pure helium gas was used as a carrier with a continuous flow rate. For detection, an injection volume of 10 μL was used, and mass spectra were recorded at an ionizing energy of 70 eV with the scanning range m/z 40−650. The GC/MS analysis was performed for a total of 27.09 min. In order to identify the potential bioactive compounds present in the EA extract of *C. gloeosporioides*, the MS spectra obtained from GC/MS analysis were compared with the known compounds stored in the NIST 2.0 MS library (National Institute of Standards and Technology, USA).

DNA Damage Protection Assay. The DNA damage protection assay is based on the inhibitory activity of the EA

https://doi.org/10.1021/acsomega.2c05746
ACS Omega 2023, 8, 3768−3784

extract of *C. gloeosporioides* against hydroxyl radicals generated by Fenton's reagent to protect the pBR322 plasmid DNA.[25] Briefly, the reaction mixture of Fenton's reagent (30 mM H_2O_2, 50 mM ascorbic acid, and 80 mM $FeCl_3$) was added to different concentrations of the EA extract of *C. gloeosporioides* (50, 100, and 200 μg/mL) in a ratio of 1:1 (v/v). Further, 2 μL of 0.5 μg of pBR322 plasmid DNA was added to the reaction mixture, and the volume was maintained up to 20 μL by using nuclease-free water and incubated at 37 °C for 10 min. The positive control consists of Fenton's reagent and pBR322 plasmid DNA, whereas the negative control contains only pBR322 plasmid DNA. After incubation, the samples were loaded onto 1% agarose gel, gel electrophoresis was performed, and the image was captured in a Gel Doc EZ imager (Bio-Rad USA). The representative image and result were from three independent experiments.

Cell Culture Maintenance and *In Vitro* Cytotoxicity Assay. The cytotoxic activity of the EA extract of *C. gloeosporioides* was performed using the 3-(4,5-dimethylthiazol-2-yl)-2,5-diphenyl tetrazolium bromide (MTT) assay.[26] Invasive ductal/breast carcinoma cells, MDA-MB-231 and MCF-7, were grown in Dulbecco's modified Eagle's medium (Himedia) with 10% heat-inactivated fetal bovine serum (HI-FBS, Thermo Fisher Scientific) in a T-25 flask and were passaged using trypsin−EDTA (Himedia, TCL034) upon 80−90% of cell confluency. The cells were maintained in a 5% CO_2 incubator at 37 °C and observed daily for cellular morphology and the presence of any contaminations.

To perform the MTT assay, 1×10^4 cells/well were seeded in a 96-well plate and incubated overnight at 37 °C in a 5% CO_2 incubator. Following incubation, the EA extract of *C. gloeosporioides* with concentration ranges of 5−100 and 10−500 μg/mL was used for MDA-MB-231 and MCF-7 cells, respectively, for 24 h, while the 0.1% DMSO (Merck)-treated cells were used as vehicle control. Post-incubation, 5 mg/mL of the MTT (SRL) per well was added and incubated for 4 h at 37 °C. The resulting formazan crystals were dissolved in 50 μL of DMSO, and the absorbance was recorded at 570 nm using a Multiskan microplate spectrophotometer (Thermo Fisher Scientific, USA) after 10 min of incubation. The results of the cytotoxic assay were expressed as the cell viability percentage against the vehicle control group, which was calculated using the formula [($Abs_{(570nm)}$ of the treated sample/$Abs_{(570nm)}$ of vehicle control)] × 100. The representative result was from three independent experiments, and the IC_{30}, IC_{50} and IC_{70} values of the EA extract of *C. gloeosporioides* for each cell were calculated using GraphPad Prism (version 8.0.2) by using the straight line curve method, followed by the interpolation of *X*-axis value. The concentrations of the EA extract of *C. gloeosporioides* needed to kill 30, 50, and 70% of the cancer cells are represented by the IC_{30}, IC_{50}, and IC_{70} values, respectively.

Evaluation of Colony-Forming Ability. The clonogenic assay was carried out to evaluate the long-term effect of the EA extract of *C. gloeosporioides* on colony-forming ability of human breast cancer cells MDA-MB-231 and MCF-7.[27] Briefly, MDA-MB-231 and MCF-7 cells were seeded at a density of 1×10^3 cells per well in a six-well plate for 24 h. Post-incubation, human breast cancer cells, MDA-MB-231 and MCF-7, were treated with different concentrations of the EA extract of *C. gloeosporioides* (IC_{30}, IC_{50}, and IC_{70}). Post-treatment, the cells were allowed to grow in culture media with repeated change of fresh media after 2 days for up to 14 days. On the 14th day, the cells were stained with 0.1% crystal violet (diluted in methanol) after being fixed in ice-cold 70% methanol. The obtained colonies were counted using ImageJ 1.53e software considering the colonies of the vehicle control group as 100%. The representative image and result were from three independent experiments.

Wound Healing Assay. An *in vitro* wound healing assay was under low serum (2% FBS) condition to assess the impact of the EA extract of *C. gloeosporioides* on cell migration ability of human breast cancer cells MDA-MB-231 and MCF-7 following the method described previously.[28] Briefly, human breast cancer cells, MDA-MB-231 and MCF-7, were seeded at a density of 2×10^5 cells per well in a six-well plate to form a continuous monolayer. Thereafter the formation of a monolayer, a uniform wound was created by scratching the cells with a sterile 20−200 μL micropipette tip. Now, the cells were washed gently with 1X sterile PBS to remove the cell debris, followed by treatment with different concentrations of the EA extract of *C. gloeosporioides* (IC_{30}, IC_{50}, and IC_{70}). Then, the image of the same scratch area was captured at 0 and 24 h under an inverted microscope (ZEISS Axio Vert A1) mounted with a digital camera. The length of the cell-free areas was measured using ImageJ software, and cell migration was calculated for the effectiveness of the EA extract of *C. gloeosporioides* in terms of recovery percentage (% *R*) using the following equation

$$\%\ R = [1 - (\text{wound length at } T_{24h}/\text{wound length at } T_{0h})] \times 100$$

where T_{0h} is the wound length at 0 h and T_{24h} is the wound length at 24 h after creating wound. The results were representative of three independent experiments.

Nuclear Morphometric Analysis Using DAPI Staining. DAPI, a fluorescence dye staining was used to evaluate the presence of apoptotic cells and nuclear morphology of breast cancer cells MDA-MB-231 and MCF-7 treated with the EA extract of *C. gloeosporioides*.[26] Briefly, the human breast cancer cells, MDA-MB-231 and MCF-7, were seeded in a six-well plate containing a coverslip at a density of 1×10^5 cells and treated with the EA extract of *C. gloeosporioides* (IC_{30}, IC_{50}, and IC_{70}), and after 24 h, the cells were fixed with paraformaldehyde at room temperature, followed by incubation with 70% methanol for 30 min in −20 °C. Post-incubation, the cells were stained with DAPI (Puregene, Genetix) for 10 min at room temperature, and the image was captured using a fluorescence microscope (Leica, Germany). The representative image was from three independent experiments.

Annexin V-FITC/PI Staining for Quantitative Assessment of Apoptosis. Quantitative assessment of the EA extract of *C. gloeosporioides*-induced apoptosis in MDA-MB-231 and MCF-7 cells was analyzed using the Dead Cell Apoptosis Kit (Thermo Fisher Scientific) containing Annexin V-FITC and propidium iodide (PI).[29] Briefly, MDA-MB-231 and MCF-7 cells were seeded at a density of 2×10^5 cells per well in a six-well plate for 24 h and then treated with the EA extract of *C. gloeosporioides* and tamoxifen (positive control) with respective IC_{50} values. Post 24 h of treatment, MDA-MB-231 and MCF-7 cells were trypsinized and rinsed with cold 1X PBS, and 1×10^5 cells were resuspended in Annexin binding buffer. The resuspended cells were incubated with 5 μL of Annexin V-FITC and 1 μL of PI (100 μg/mL) at room temperature for 15 min in the dark condition. Post-incubation,

https://doi.org/10.1021/acsomega.2c05746
ACS Omega 2023, 8, 3768−3784

50,000 cells were analyzed through flow cytometry (BD LSR Fortessa, BD Biosciences, USA), and quantification was performed through FlowJo software. The representative result was from three independent experiments.

Evaluation of ROS Generation by Fluorimetric Assay. The level of cellular ROS induced by the EA extract of *C. gloeosporioides* in human breast cancer cells MDA-MB-231 and MCF-7 was evaluated using the 2′, 7′-dichlorofluorescein diacetate (H2DCFDA) dye-based assay as described previously.[30] Briefly, human breast cancer cells, MDA-MB-231 and MCF-7, at a density of 2×10^5 cells were treated with the EA extract of *C. gloeosporioides* with a respective IC_{50} value for 24 h. The treated cells were harvested and homogenized in 1X PBS, followed by centrifugation at 10,000*g* at 4 °C. The supernatant containing cellular ROS was collected and quantified using a NanoDrop ONE (Thermo Scientific, USA). Further, an equal quantity of protein was incubated with 2 mM 2′,7′-dichlorofluorescein diacetate (H2DCFDA) for 30 min at 37 °C. The available ROS converted the non-fluorescent H2DCFDA to highly fluorescent 2′,7′-dichlorofluorescein (DCF), which was recorded at an excitation wavelength of 488 nm and an emission wavelength of 525 nm using a multimode reader (Thermo Scientific, USA). The level of cellular ROS in each sample was determined by calculating the fluorescence intensity value per milligram of protein. The representative result was from three independent experiments.

Evaluation of Mitochondrial Membrane Potential (ΔΨmt). The mitochondrial membrane potential (MMP or ΔΨm) was measured using the cationic carbocyanine dye rhodamine 123 (Rh 123) as done previously, with minor modification.[31] The healthy mitochondria with normal ΔΨm give increased fluorescence intensity due to sequestering of a higher amount of Rh 123. Briefly, MDA-MB-231 and MCF-7 cells were seeded at a density of 2×10^5 cells per well in a six-well plate and incubated for confluency up to 70−80%. Post-incubation, the cells were treated with the EA extract of *C. gloeosporioides* with respective IC_{50} values for 24 h. Mitochondrial cells were isolated from the cells of vehicle control (0.1% DMSO) and treated (with IC_{50} value of the EA extract of *C. gloeosporioides*) groups in mitochondrial isolation buffer (225 mM mannitol, 75 mM sucrose, 5 mM HEPES, 1 mM EGTA, 1 mg/mL BSA, and pH 7.4), as described previously.[32] The pellet containing mitochondria was suspended in the mitochondrial isolation buffer without EGTA, and protein was estimated. An equal quantity of mitochondria from each group was taken and incubated with 0.3 μM Rh 123 dye for 25 min at 37 °C, and fluorescence was recorded in the multimode reader at wavelengths of 535 nm (excitation) and 580 nm (emission). The fluorescence intensity value was used to reflect the MMP. The representative result was from three independent experiments.

RNA Isolation and Quantitative Reverse Transcription—Polymerase Chain Reaction. The antiproliferative mechanism induced by the EA extract of *C. gloeosporioides* in cancer cells MDA-MB-231 and MCF-7 was validated by evaluating the relative gene expression level of marker of cancer cell stemness (*CD44*), pro-apoptotic (*BAX*, *PARP*, *CASPASE-8*, and *FADD*), antiapoptotic (*BCL-2* and *SURVIVIN*), cell cycle inhibitor (*P21*), and tumor suppressor (*P53*) genes using qRT-PCR analysis. The sequence of primers set for each gene is given in Table S1. β-Actin was used as an internal control for normalization. The standard guideline of MIQE was followed for all the essential quantitative reverse transcription−polymerase chain reaction (qRT-PCR) information.[33] Briefly, human breast cancer cells MDA-MB-231 and MCF-7 were seeded at a density of 2×10^5 cell per well in a six-well plate and incubated overnight for 70−80% confluency. After 24 h, the cells were treated with respective IC_{50} values for next 24 h. After 24 h, total RNA was isolated using the TRIZOL method from the cells of vehicle control (0.1% DMSO) and treated (with IC_{50} value of EA extract of *C. gloeosporioides*) groups. The concentration and purity of the extracted RNA were measured using the NanoDrop ONE (AZY1811395, Thermo Scientific, USA). RNA (5 μg) from each group was reverse-transcribed into cDNA using the RevertAid First-Strand cDNA Synthesis Kit (Thermo Fisher Scientific, USA) according to the manufacturer's protocol with minor modifications.[34] Further, the synthesized cDNA was used as a template to perform qRT-PCR (QuantStudio 5 Real-Time PCR System) using gene-specific primers and the PowerUp SYBR Green master mix (Thermo Fisher Scientific, USA). Data for qRT-PCR was analyzed by the ΔΔCT comparative method, and relative mRNA expression level was calculated in terms of fold change using the $2^{-\Delta\Delta CT}$ method. The representative result was from three independent experiments.

Caspase-3 Activity Assay. The Caspase-3 activity in breast cancer cells, MDA-MB-231 and MCF-7, was examined using the Caspase 3 Activity Assay Kit (Elabscience, E-CK-A311A) following the manufacturer's protocol. Briefly, MDA-MB-231 and MCF-7 cells were seeded in a six-well plate at a density of 2×10^5 cells and incubated overnight for 70−80% confluency. Post-incubation, the cells were treated with respective IC_{50} value of the EA extract of *C. gloeosporioides* for 24 h. Post-treatment, the cells was trypsinized and washed once with cold 1X PBS to remove excess culture media and trypsin. Further, the cells were lysed with lysis buffer (containing DTT) for 30 min at 4 °C and centrifuged at 12,000 rpm for 15 min at 4 °C. The supernatant containing Caspase-3 protein was collected, and the reaction mixture was prepared by adding the protein sample, reaction buffer, and substrate Ac-DEVD-pNA at a final volume of 100 μL and incubated at 37 °C for 4 h. Post-incubation, the absorbance was recorded at 405 nm using a Multiskan microplate spectrophotometer (Thermo Fisher Scientific, USA), and the fold change in the activity of Caspase-3 was calculated. The representative result was from three independent experiments.

Protein Isolation and Immunoblotting. The expression level of antiapoptotic protein Bcl-2 was evaluated by immunoblotting, as described previously with minor modification.[35] Briefly, the MDA-MB-231 and MCF-7 cells were seeded at a density of 2×10^5 cell per well in a six-well plate and incubated overnight at 37 °C in a 5% CO_2 incubator. After the formation of a monolayer, each cell was treated for 24 h. Post-treatment, the cells were washed with PBS, followed by lysis in 500 μL of lysis buffer [20 mM Tris-Cl (pH 8.0), 137 mM NaCl, 10% (v/v) glycerol, 1% (v/v) Triton X-100, 2 mM EDTA, 1 mM phenylmethylsulfonyl fluoride, and 20 μM leupeptin containing aprotinin at 0.15 U/mL]. The protein concentration was quantified by the standard Bradford method.[36] Thereafter, an equal concentration of cellular proteins of each sample was resolved on SDS-polyacrylamide gel by electrophoresis. The resolved proteins were transferred to the nitrocellulose membrane (Axiva, New Delhi, India), immunoblotted with primary antibodies of Bcl-2, and proceeded by probing with a corresponding secondary

https://doi.org/10.1021/acsomega.2c05746
ACS Omega 2023, 8, 3768−3784

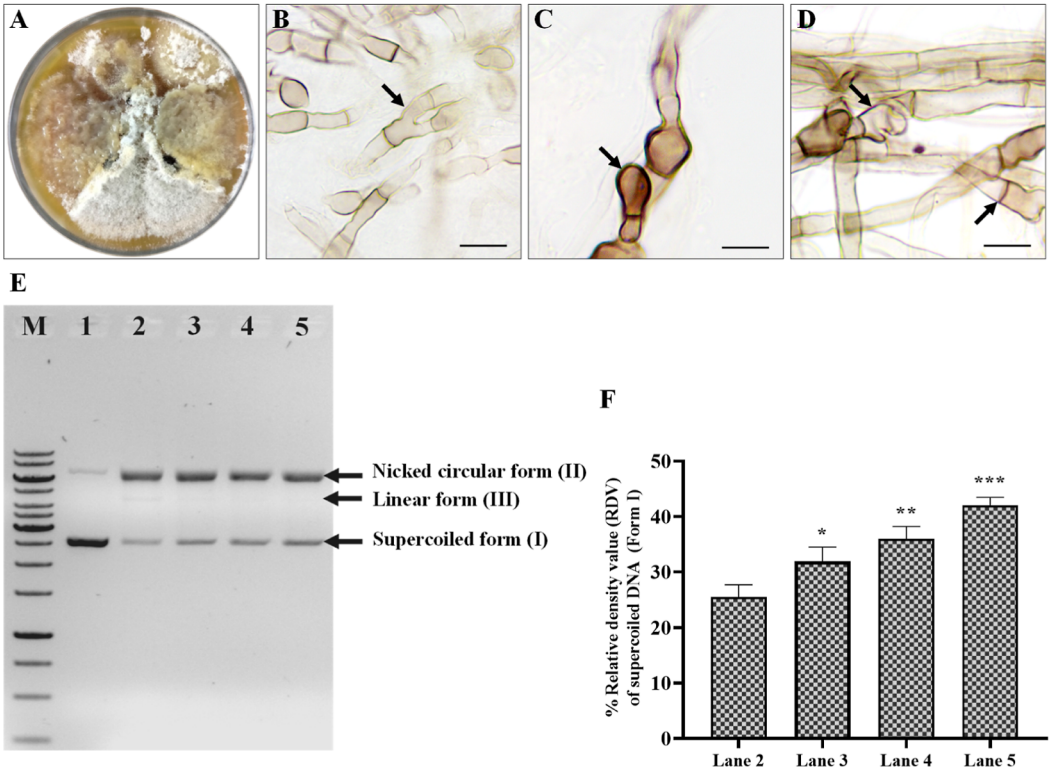

Figure 1. Morphological characteristics of the fungal endophyte *C. gloeosporioides* and the *in vitro* DNA protective activity of the EA extract of *C. gloeosporioides*. (A) Colony of *C. gloeosporioides* on the PDA plate after 10 days at 27 °C, (B) mycelia, (C) germinating conidia and forming appressoria, and (D) mycelial septa and Appressoria. Scale bar = 100 μm. (E) Gel electrophoresis pattern showing the protective effect of the EA extract of *C. gloeosporioides* for pBR322 plasmid DNA against hydroxyl radicals generated from Fenton's reagent. M: 1 kb Ladder; Lane 1: DNA (plasmid pBR322 alone); Lane 2: plasmid DNA treated with Fenton's reagent; Lane 3: plasmid DNA treated with Fenton's reagent and the EA extract of *C. gloeosporioides* (50 μg/mL); Lane 4: plasmid DNA treated with Fenton's reagent and the EA extract of *C. gloeosporioides* (100 μg/mL); and Lane 5: plasmid DNA treated with Fenton's reagent and the EA extract of *C. gloeosporioides* (200 μg/mL). (F) Histogram represents the percent RDV of the supercoiled form (I) of plasmid DNA recovered after treatment with the EA extract of *C. gloeosporioides*. Statistical significance (***, $p < 0.001$; **, $p < 0.010$; and *, $p < 0.050$) was calculated by performing independent Student's *t*-test and compared the mean ± SD of the EA extract of *C. gloeosporioides* treated group with the control group (plasmid Fenton's reagent alone treated).

antibody conjugated to alkaline phosphatase substrates, followed by detection of protein bands by incubating in BCIP/NBT solution. The intensity of bands was quantified by "ImageJ" software (NIH USA). β-Actin was used as a loading control. The representative result was from three independent experiments.

Statistical Analysis. In the current study, all the experiments for each group were performed in triplicate (n = 3). Data for the DNA damage protective assay, cytotoxicity assay, colony formation assay, wound healing assay, Annexin V-FITC/PI staining, ROS, MMP, and Caspase-3 activity were presented as mean ± SD in histogram. For the statistical significance of cytotoxicity and Annexin V-FITC/PI staining, one-way ANOVA (analysis of variance) followed by Tukey's test was performed, and the mean ± SD of each group was compared with all other groups using Graph Pad Prism 8.0.2 software, whereas the mean ± SD of the EA extract of *C. gloeosporioides* treated group for the data of DNA damage protective assay, colony formation assay, wound healing assay, ROS, MMP, and Caspase-3 activity was compared with the respective vehicle control group, and statistical significance was calculated by performing independent Student's *t*-test, followed by using SPSS 16.0 software. For qRT-PCR data normalization, the ΔΔCT value was determined to evaluate the relative mRNA expression in terms of fold change by the $2^{-\Delta\Delta CT}$ method. Statistical significance of qRT-PCR and immunoblotting data were evaluated by comparing the means ± SEM and mean ± SD, respectively, of vehicle control and the EA extract of *C. gloeosporioides* treated group by independent Student's *t*-test, followed by using SPSS 16.0 software. For graphical representation, the histogram of all experiments was plotted in Graph Pad Prism 8.0.2 software.

RESULTS AND DISCUSSION

GC/MS Analysis Reveals the Presence of 35 Compounds in the EA Extract of *C. gloeosporioides*. *C. gloeosporioides* (accession number LC585212) (Figure 1A–D) associated with the leaf of *O. indicum* plant is already reported to produce bioactive metabolites which show good antioxidant and cytotoxic activities.[23] In the present study, we were interested to elucidate the molecular mechanism of the anticancer role of bioactive compounds produced from *C. gloeosporioides* in human breast cancer cells. To address this, we first performed GC/MS for the identification of bioactive compounds present in the EA extract of fungal strain *C. gloeosporioides*. A total of 35 major compounds were identified from the fungal extract of *C. gloeosporioides* along with their respective molecular formula, molecular weight, and previously reported biological activities (Table 1). A total of nine major bioactive compounds with prominent relative area percentage were detected as 8-methyl-6-nonenamide (12.25%), dodecanamide (9.66%), 4-hydroxy-2-butanone (9.54%), 7-nonena-

https://doi.org/10.1021/acsomega.2c05746
ACS Omega 2023, 8, 3768−3784

Table 1. List of Major Compounds Identified through GC/MS Analysis of the EA Extract of the Fungal Endophyte *C. gloeosporioides*

s. no.	retention time	compound name	molecular weight (g/mole)	molecular formula	biological activity	relative area %
1	3.06	4-hydroxy-2-butanone	88.11	$C_4H_8O_2$		9.54
2	3.60	*cis*-1,4-diacetoxy-2-butene	172.18	$C_8H_{12}O_4$		2.98
3	3.86	2-butene-1,4-diol, diacetate	172.18	$C_8H_{12}O_4$		6.53
4	4.12	1,2,5-oxadiazole	70.05	$C_2H_2N_2O$	antiproliferative activity and antiparasitic activity	9.01
5	4.35	4-fluoro-4-methylpentane-2,3-dione	132.13	$C_6H_9FO_2$		6.92
6	5.77	pyrrolidine	71.12	C_4H_9N	free radical scavenger, anti-inflammatory activity, and antitumor activity	0.57
7	6.62	hexane, 3,3-dimethyl-	114.23	C_8H_{18}	antioxidant activity	1.39
8	7.29	heptane, 2,4-dimethyl-	128.25	C_9H_{20}		1.31
9	8.66	1-fluorononane	146.25	$C_9H_{19}F$	anticancer activity (in silico docking study)	0.74
10	8.78	oxalic acid, isobutyl pentyl ester	216.27	$C_{11}H_{20}O_4$	antioxidant activity	1.17
11	9.52	benzene, 1,3-bis(1,1-dimethylethyl)-	190.32	$C_{14}H_{22}$	lipid oxidation	0.54
12	9.87	undecane, 4,7-dimethyl-	184.36	$C_{13}H_{28}$		1.02
13	10.51	undecane	156.31	$C_{11}H_{24}$	sex pheromones	0.64
14	11.46	9-octadecene, (E)-	252.5	$C_{18}H_{36}$	antifungal activity, antioxidant activity, anticarcinogenic activity, and antimicrobial activity	0.64
15	11.56	tridecane	184.36	$C_{13}H_{28}$	antimicrobial activity	0.64
16	11.70	2,4,6,8-tetramethyl-1-undecene	210.4	$C_{15}H_{30}$	antibiotic activity	0.69
17	12.38	dodecane, 2,6,11-trimethyl-	212.41	$C_{15}H_{32}$	antibacterial activity	0.81
18	12.71	undecane, 3,8-dimethyl-	184.36	$C_{13}H_{28}$	antioxidant activity	1.43
19	13.28	dodecane, 4,6-dimethyl-	198.39	$C_{14}H_{30}$	antibacterial activity	0.99
20	13.97	9-eicosene, (E)-	280.5	$C_{20}H_{40}$	antimicrobial activity and cytotoxic activity	1.04
21	15.24	hexadecane	226.44	$C_{16}H_{34}$	antibacterial, antifungal, and antioxidant activities	1.04
22	15.73	1-iodo-2-methylundecane	296.23	$C_{12}H_{25}I$	antimicrobial activity	0.62
23	16.14	8-methyl-6-nonenamide	169.26	$C_{10}H_{19}NO$		12.25
24	16.38	7-nonenamide	155.24	$C_9H_{17}NO$	antioxidant activity	9.28
25	16.55	dodecanamide	199.33	$C_{12}H_{25}NO$	antibacterial activity	9.66
26	17.50	2-bromotetradecane	277.28	$C_{14}H_{29}Br$		1.04
27	18.29	heptadecanoic acid, heptadecyl ester	508.9	$C_{34}H_{68}O_2$	antioxidant activity and antifungal activity	1.17
28	19.99	1-(2,6-dichlorophenyl)-1,3-dihydro-2H-indol-2-one	278.1	$C_{14}H_9Cl_2NO$	non-steroidal, anti-inflammatory activity	1.21
29	20.18	octadecane, 1-(ethenyloxy)-	296.5	$C_{20}H_{40}O$	antisepsis	0.58
30	20.83	benzene, 1,1′-sulfonylbis [4-chloro-	287.2	$C_{12}H_8Cl_2O_2S$		0.75
31	21.65	eicosanoic acid, phenylmethyl ester	402.7	$C_{27}H_{46}O_2$	anti-inflammatory activity and antibacterial activity	0.99
32	22.66	phenol, 2,2′-methylenebis[6-(1,1-dimethylethyl)-4-methyl	340.5	$C_{23}H_{32}O_2$	antioxidant activity	0.57
33	24.21	hexadecanoic acid, 2-hydroxy-1-(hydroxymethyl)ethyl ester	330.5	$C_{19}H_{38}O_4$	antioxidant activity, anti-inflammatory activity, and anthelmintic activity	2.45
34	24.48	phthalic acid, 4-methylhept-3-yl octadecyl ester	530.8	$C_{34}H_{58}O_4$	antibacterial activity	1.23
35	25.24	11,13-dimethyl-12-tetradecen-1-ol acetate	282.5	$C_{18}H_{34}O_2$	antituberculosis activity	0.50

mide (9.28%), 1,2,5-oxadiazole (9.01%), 4-fluoro-4-methylpentane-2,3-dione (6.92%), 2-butene-1,4-diol, diacetate (6.53%), *cis*-1,4-diacetoxy-2-butene (2.98%), and hexadecanoic acid (2.45%). Besides, other bioactive compounds such as pyrrolidine, hexane, 3,3-dimethyl-; oxalic acid, isobutyl pentyl ester; 2,4,6,8-tetramethyl-1-undecene; undecane, 3,8-dimethyl-; dodecane, 4,6-dimethyl-; 1-(2,6-dichlorophenyl)-1,3-dihydro-2*H*-indol-2-one; benzene, 1,1′-sulfonylbis[4-chloro-; eicosanoic acid, phenylmethyl ester; and phenol, 2,2′-methylenebis[6-(1,1-dimethylethyl)-4-methyl] were also found.

The result of GC/MS analysis of the EA extract of *C. gloeosporioides* (Table S2) shows that the fungal endophyte *C. gloeosporioides* is capable of producing structurally diverse bioactive compounds and can be useful for the development of natural bioactive compounds with antioxidant and anticancer activities. The EA extract of *C. gloeosporioides* also contains several compounds with anticancer and antiproliferative properties such as 9-eicosene, (E)-; 9-octadecene, (E)-; 1-fluorononane; and 1,2,5-oxadiazole, which evidenced the cytotoxic property of the fungal extract of *C. gloeosporioides*. A previous study showed the production of the anticancer compound piperine, which was isolated from the fungal species *C. gloeosporioides* associated with the plant *Piper nigrum*.[37,38] Bioactive compounds 8-methyl-6-nonenamide; thiophen-2-ylmethylenehydrazide; benzene, 1,1′-sulfonylbis [4-chloro-; 4-hydroxy-2-butanone; *cis*-1,4-diacetoxy-2-butene; 2-butene-1,4-diol, diacetate; 4-fluoro-4-methylpentane-2,3-dione; heptane, 2,4-dimethyl-; and undecane, 4,7-dimethyl- were reported in the previous literature, however not studied for their antioxidant, cytotoxic, and antibacterial activities, which complement further credibility to the current study. GC/MS results also suggest the presence of a non-steroidal anti-inflammatory compound; 1-(2,6-dichlorophenyl)-1,3-dihydro-

https://doi.org/10.1021/acsomega.2c05746
ACS Omega 2023, 8, 3768−3784

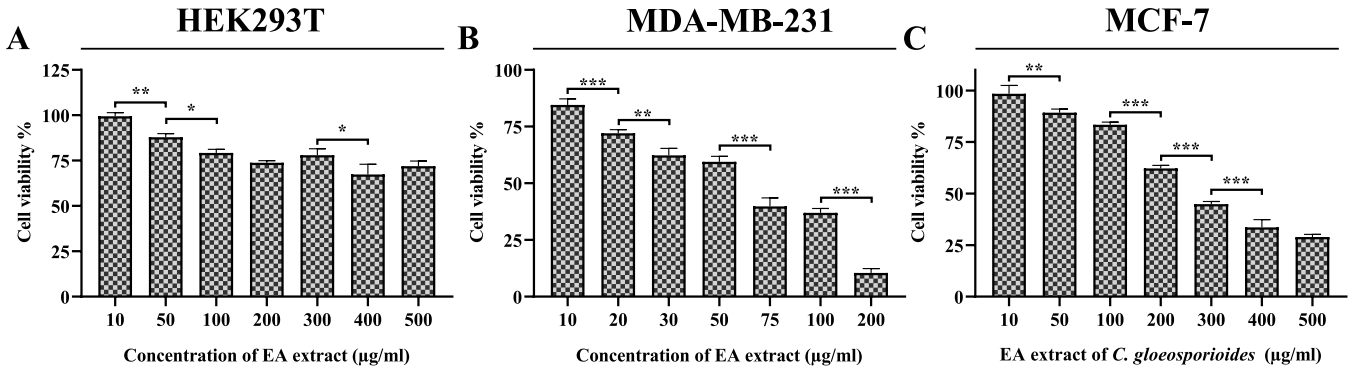

Figure 2. Cytotoxic activity of the EA extract of *C. gloeosporioides* against (A) non-cancerous, HEK293T, and human breast cancer cells (B) MDA-MB-231 and (C) MCF-7. All experiments were performed in triplicate. *p*-value was calculated by comparing the mean ± SD of the percentage of cell viability using one-way ANOVA, followed by Tukey's test to determine the statistical significance. The statistical significance is as follows: ***, $p \leq 0.001$; **, $p \leq 0.002$; and *, $p \leq 0.033$.

2H-indol-2-one is produced from the fungal endophyte *C. gloeosporioides*. Moreover, the non-steroidal anti-inflammatory drugs (NSAIDs) are reported to possess anticancer property. For example, aspirin is a well-known NSAID with potential anticarcinogenic effect used in the treatment of gastrointestinal tract cancer.[39] GC/MS analysis revealed the presence of various bioactive compounds in the EA extract of the fungal endophyte *C. gloeosporioides* with anticancer properties. Therefore, the DNA damage protection activity against pBR322 and the anticancer role of the EA extract of *C. gloeosporioides* were evaluated against two human breast cancer cells MDA-MB-231 and MCF-7.

EA Extract of *C. gloeosporioides* Shows the Potential DNA Protective Activity. The pBR322 plasmid DNA damage protection activity of the EA extract of *C. gloeosporioides* was evaluated by the DNA nicking assay. Lane 1 (Figure 1E) showed only plasmid DNA pBR322 with two distinct bands of supercoiled form (form I), and lane 2 showed the nicking effect of Fenton's reagent. Fenton's reagent caused nicking of plasmid DNA pBR322 into small pieces, and therefore, three nicked forms, supercoiled form (form I), nicked circular form (form II), and double-stranded nicked linear form (form III), were observed, whereas different concentrations of the EA extract of *C. gloeosporioides*, that is, 50, 100, and 200 μg/mL, were added in the solution of DNA pBR322, and Fenton's reagent prevented the radical-induced DNA damage and disappearance of nicked linear form DNA (form III) in a concentration-dependent manner. The relative density value (RDV) (Figure 1F) of supercoiled form DNA (form I) was observed to be restoring at a concentration of 200 μg/mL and moving closer to the supercoiled form of plasmid DNA of lane 1. The result of percentage of RDV of supercoiled DNA form I at 50, 100, and 200 μg/mL was 31.93 ± 2.587% (*t*-value −3.28; *p*-value 0.031), 36.02 ± 2.201% (*t*-value −5.86; *p*-value 0.004), and 42.03 ± 1.446% (*t*-value −10.89; *p*-value 0.000), respectively. Therefore, the results suggest the restoration of the native form of plasmid DNA to form I with increasing concentration of the EA extract of *C. gloeosporioides*. The DNA protective effect of the EA extract of *C. gloeosporioides* can be due to the high phenolic content and that attributed to the antioxidant potential of the EA extract of *C. gloeosporioides*. The protective activity of the EA extract of *C. gloeosporioides* for pBR322 plasmid DNA caused by hydroxyl radicals of Fenton's reagent shows a linear relationship with the antioxidant ability of the EA extract of *C. gloeosporioides* against synthetically generated free radicals DPPH, $O_2^{-\bullet}$, $^{\bullet}NO$, and $^{\bullet}OH$.[23]

DNA, the fundamental component and genetic material of all living organisms, is remarkably vulnerable to damage from both intracellular and extracellular factors; however, the intracellular factors including free radicals tend to cause damage more frequently than the external ones. Here, we performed *invitro* study to examine the ability of the EA extract of *C. gloeosporioides* to protect DNA against the damage caused by synthetically produced hydroxyl radicals, which behave similarly to the endogenous ROS. Our *in vitro* findings revealed that the EA extract of *C. gloeosporioides* attenuated the negative impact of Fenton's reagent-generated hydroxyl radicals on the plasmid DNA pBR322 in a concentration-dependent manner. The pBR322 plasmid DNA found mainly in the supercoiled form (form I). Treatment of plasmid DNA with Fenton's reagent leads to the formation of a single-stranded nicked circular form (form II) and double-stranded nicked linear DNA (form III). Exposure of plasmid DNA to Fenton's reagent causes strand breaks in DNA due to the attack of $^{\bullet}OH$ radicals generated in the reaction mixture. When hydroxyl radicals react with DNA, nitrogenous bases of DNA produce base radicals and sugar radicals. These base radicals react with the sugar moiety, causing breakage of the sugar-phosphate backbone of nucleic acid resulting in strand break. The DNA protective activity of the EA extract of *C. gloeosporioides* attributed to the synergistic effect of antioxidant compounds, whose presence was validated by GC/MS analysis.

EA Extract of *C. gloeosporioides* Shows Significant Cytotoxic Activity against Human Breast Cancer Cells. Since there are still a lot of unmet medical needs in cancer therapies, novel natural therapeutic agents are needed. Globally, breast cancer (BC) is one of the most prevalent cancers that affects women and reported to surpass lung cancer. According to epidemiological studies, it is expected that there would be over 2.3 million new cases of breast cancer by the year 2030.[40] In light of the widespread prevalence of human breast cancer and the need to investigate bioactive compounds derived from the endophyte *C. gloeosporioides*, we performed the MTT test to evaluate the cytotoxic potential of the EA extract of *C. gloeosporioides* against non-cancerous cell HEK293T (Figure 2A), the triple-negative human breast cancer MDA-MB-231 (Figure 2B), and the single-negative breast cancer MCF-7 cells (Figure 2C). The EA extract of *C. gloeosporioides* exhibited potential cytotoxicity against both

https://doi.org/10.1021/acsomega.2c05746
ACS Omega 2023, 8, 3768−3784

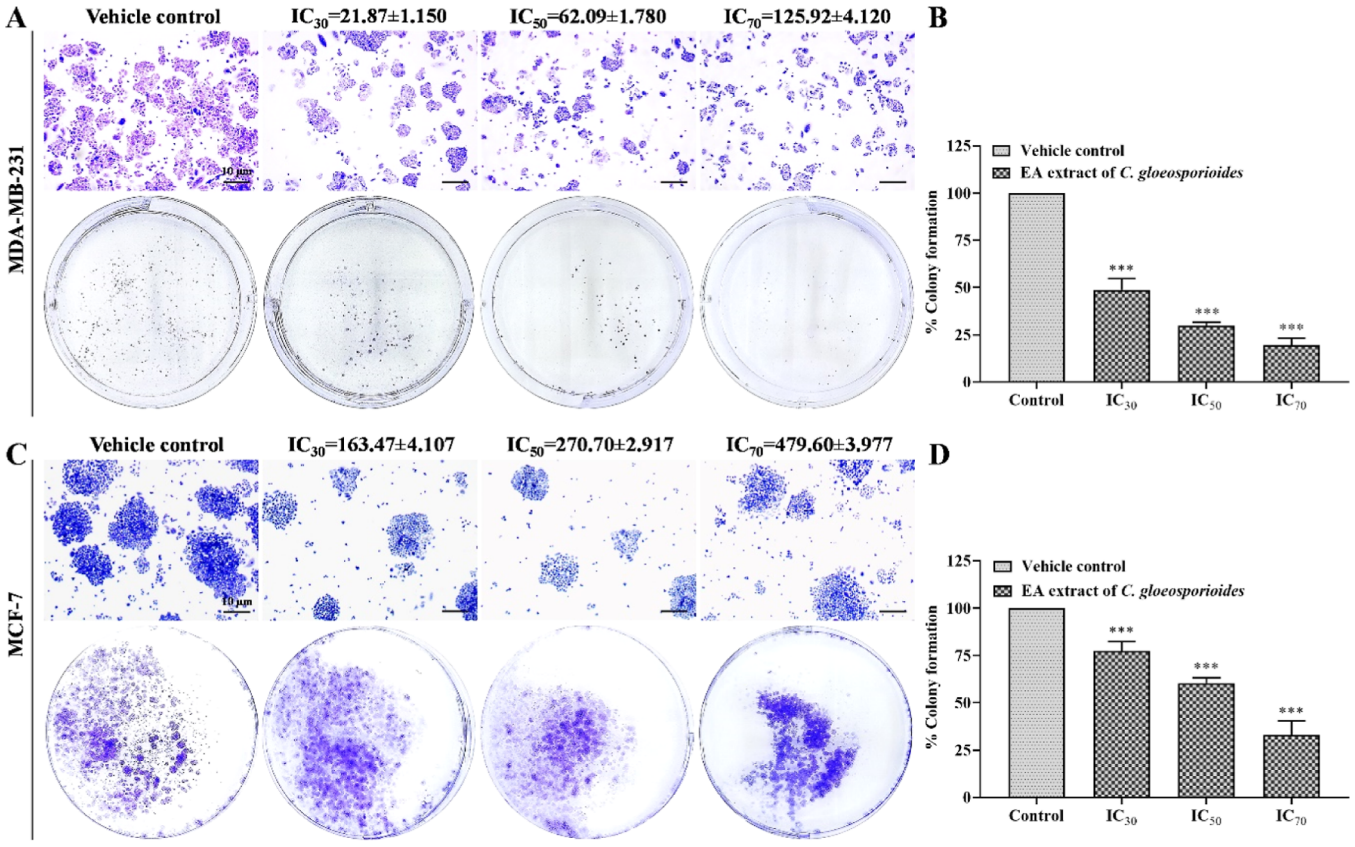

Figure 3. EA extract of *C. gloeosporioides* induces the inhibition of the colony-forming ability of MDA-MB-231 and MCF-7 cells. (A) Images of the colony formed by MDA-MB-231 in vehicle control and the EA extract of *C. gloeosporioides* treated group (IC_{30}, IC_{50}, and IC_{70}) in six-well plates and their respective microscopic images (scale bar = 10 μm). (B) Histogram of % colony formed by MDA-MB-231 cells (C). Images of the colony formed by MCF-7 in vehicle control and the EA extract of *C. gloeosporioides* treated group (IC_{30}, IC_{50}, and IC_{70}) in six-well plates and their respective microscopic images (scale bar = 10 μm). (D) Histogram of % colony formed by MCF-7 cells. Data are presented as mean ± SD of the colony formed by cancer cells (n = 3), and p-value was calculated using independent Student's t-test to determine the statistical significance. The statistical significance is as follows: ***, $p < 0.001$; **, $p < 0.010$; and *, $p < 0.050$.

cancer cells MDA-MB-231 and MCF-7 with IC_{50} values of 62.09 ± 1.780 and 270.70 ± 2.917 μg/mL, respectively, whereas the EA extract of *C. gloeosporioides* did not show any obvious toxicity against HEK293T, a non-cancerous cell.

Considering the widespread prevalence of breast cancer, there is an urgent demand for natural bioactive compounds that are less toxic and more effective. The bioactive compounds derived from fungal endophytes offer a wide range of applications in the treatment of various diseases, including cancer.[41] In contrast to MCF-7 cells which are positive for estrogen (ER) and progesterone (PR) and negative for human epidermal growth factor receptors (HER-2), MDA-MB-231 cells are negative for all the three aforementioned receptors and therefore called as triple negative. In the present study, EA extract of *C. gloeosporioides* is 4 times more susceptible to MDA-MB-231 than that of MCF-7 cells in terms of cytotoxic activities. This differential susceptibility may be attributed to the different molecular microenvironments of these two breast cancer cells. Previous studies also showed that fungal metabolites and natural compounds have demonstrated non-specific cytotoxicity against breast cancer cells, including MDA-MB-231 (negative for ER, PR, and HER-2), MCF-10A (negative for ER), and MCF-7 (positive ER and PR but negative for HER-2) cells.[42,43] A recent research revealed that the EA extract of the fungal endophyte *Penicillium oxalicum* exhibits potential cytotoxic activity against human breast cancer cells MDA-MB-231 and MCF-7 with IC_{50} values of 37.24 ± 1.26 and 260.627 ± 5.415 μg/mL, respectively.[42] Therefore, the results of the current study corroborate with the previous findings, showing that breast cancer cells MDA-MB-231 and MCF-7 exhibited different susceptibility to the EA extract of *C. gloeosporioides* mediated cytotoxicity. Based on the potential cytotoxicity of the EA extract of *C. gloeosporioides*, the anticancer-based study such as the colony formation assay, wound healing assay, and nuclear morphometric analysis using DAPI staining was performed at IC_{30} (21.87 ± 1.150 μg/mL), IC_{50} (62.09 ± 1.780 μg/mL), and IC_{70} (125.92 ± 4.120 μg/mL) for MDA-MB-231 and at IC_{30} (163.47 ± 4.107 μg/mL), IC_{50} (270.70 ± 2.917 μg/mL), and IC_{70} (479.60 ± 3.977 μg/mL) for MCF-7 cells, whereas various mechanistic studies were performed in order to elucidate the molecular alteration induced by the EA extract of *C. gloeosporioides* leading to apoptosis in MDA-MB-231 and MCF-7 cells. The mechanistic studies such as quantitative analysis of apoptosis using Annexin V-FITC/PI staining, measurement of ROS and MMP, differential gene expression, immunoblotting, and Caspase-3 activity were performed at the IC_{50} value for respective human breast cancer cells.

EA Extract of *C. gloeosporioides* Significantly Inhibits the Colony-Forming Ability of Breast Cancer Cells. Cancer cells have the ability to divide and proliferate continuously to form the colony. In order to achieve a better

https://doi.org/10.1021/acsomega.2c05746
ACS Omega 2023, 8, 3768−3784

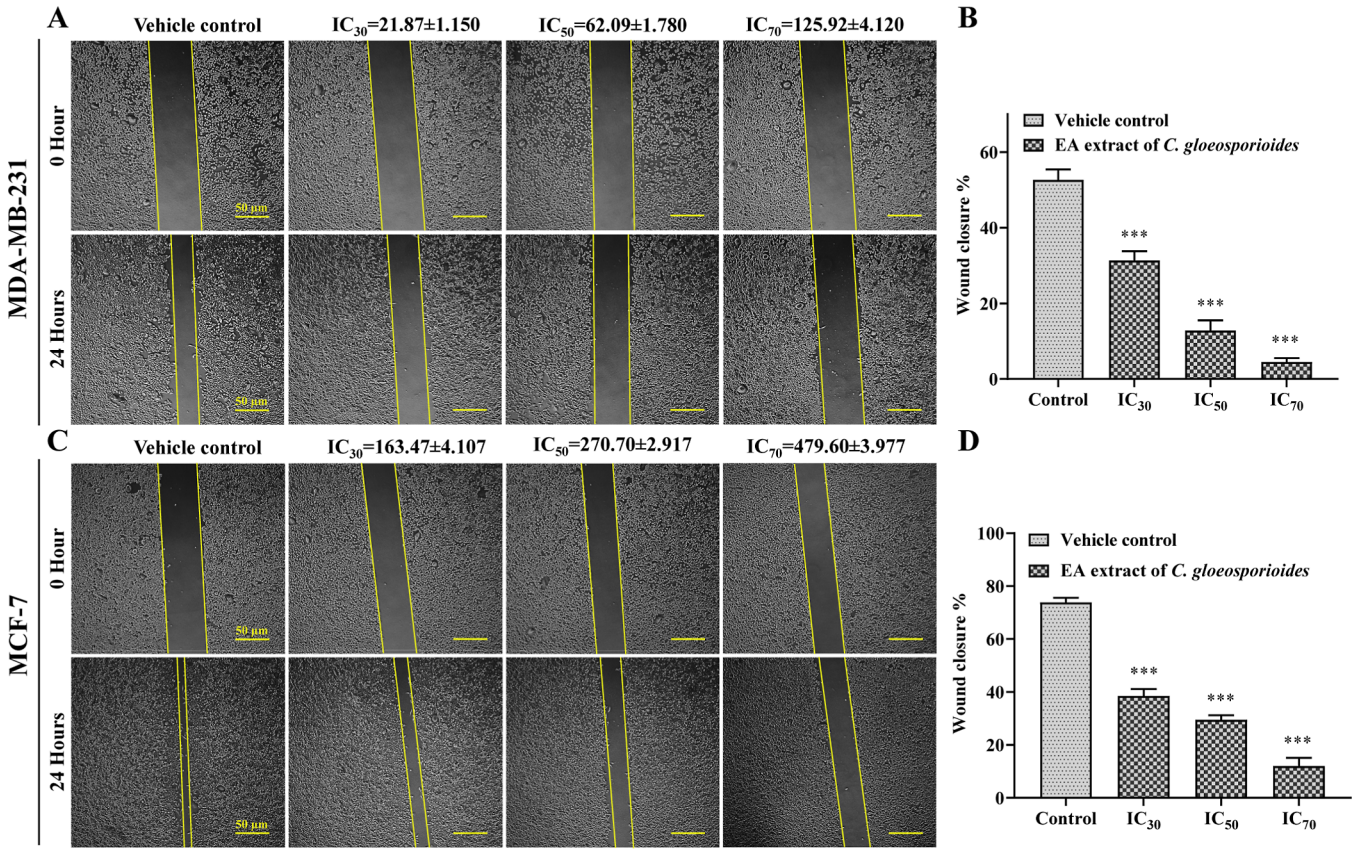

Figure 4. EA extract of *C. gloeosporioides* (IC_{30}, IC_{50}, and IC_{70}) induces the inhibition of two-dimensional cell migration ability of human breast cancer cells. (A) Microscopic image and (B) histogram of MDA-MB-231 cells showing the relative wound closure (%) after treatment with the EA extract of *C. gloeosporioides*. (C) Microscopic image. (D) Histogram of MCF-7 cells showing the relative wound closure (%) after treatment with the EA extract of *C. gloeosporioides*. *p*-value was calculated by comparing the means ± SD of percentage of wound closure in vehicle control and the EA extract of *C. gloeosporioides* treated breast cancer cells. The statistical significance (***, $p < 0.001$; **, $p < 0.010$; and *, $p < 0.050$) was calculated by performing independent Student's *t*-test. Scale bar = 50 μm.

insight into antiproliferative activity and inhibition of long-term colony-forming ability of the EA extract of *C. gloeosporioides*, an *in vitro* clonogenic assay was carried out on MDA-MB-231 (Figure 3A) and MCF-7 (Figure 3C) cells. The result of clonogenic assay showed that treatment of MDA-MB-231 cells with IC_{30}, IC_{50}, and IC_{70} values of the EA extract of *C. gloeosporioides* significantly reduced the number of colonies by 48.79 ± 5.899% (*t*-value 15.039; *p*-value 0.000), 29.80 ± 1.866% (*t*-value 65.204; *p*-value 0.000), and 19.55 ± 3.568% (*t*-value 39.047; *p*-value 0.000), respectively (Figure 3B), while the exposure of MCF-7 cells with IC_{30}, IC_{50}, and IC_{70} values of the EA extract of *C. gloeosporioides* significantly reduced the number of colonies by 77.60 ± 2.528% (*t*-value 15.339; *p*-value 0.000), 56.55 ± 3.393% (*t*-value 22.159; *p*-value 0.000), and 32.87 ± 3.203% (*t*-value 36.330; *p*-value 0.000), respectively (Figure 3D). Overall, our finding suggests that the EA extract of *C. gloeosporioides* showed reduction in the colony-forming ability of both breast cancer cells MDA-MB-231 and MCF-7.

Microscopic observation of the colony revealed that the administration of the EA extract of *C. gloeosporioides* at different concentrations also leads to a smaller number of colony as well as a reduction in colony size against both human breast cancer cells, MDA-MB-231 (Figure 3A) and MCF-7 (Figure 3C). The stemness is responsible for the metastatic behavior of the drug resistance property and recurrence of human breast cancer cells. The EA extract of the endophyte *C. gloeosporioides* inhibits the stemness property of breast cancer cells since the treatment significantly mitigated the colony-forming ability of MDA-MB-231 and MCF-7 cells. The inhibition of stemness property of the EA extract of *C. gloeosporioides* in MDA-MB-231 and MCF-7 cells was further validated through the decreased expression of *CD44* gene. The cell surface marker CD44 has been widely employed to identify cancer stem cells (CSCs) from various cancers including breast cancer.[44,45] Previous studies also suggest that in breast cancer tumorigenesis, CD44-positive cells are present that exhibit stemness characteristics such as self-renewal and differentiation. Furthermore, CD44 are known to regulate other factors such as Nanog, Oct4, and Sox2, and therefore, targeting the cell surface marker CD44 provides a better insight into the cancer stemness inhibition potential of the EA extract of *C. gloeosporioides*.[46,47] The result of relative mRNA expression showed that level of *CD44* was significantly decreased by 0.195 ± 0.092-fold (*t*-value 8.750; *p*-value 0.013) and 0.439 ± 0.042-fold (*t*-value 13.212; *p*-value 0.006) in MDA-MB-231 (Figure S1A) and MCF-7 (Figure S1B) cells, respectively. Our results clearly indicated that 24 h of exposure with IC_{30}, IC_{50}, and IC_{70} values of the EA extract of *C. gloeosporioides* significantly reduces the self-proliferation and the colony-forming ability of MDA-MB-231 and MCF-7 cells.

EA Extract of *C. gloeosporioides* Significantly Attenuates the Wound Closure Ability of Breast Cancer Cells. We further evaluated the effect of EA extract of *C.*

https://doi.org/10.1021/acsomega.2c05746
ACS Omega 2023, 8, 3768−3784

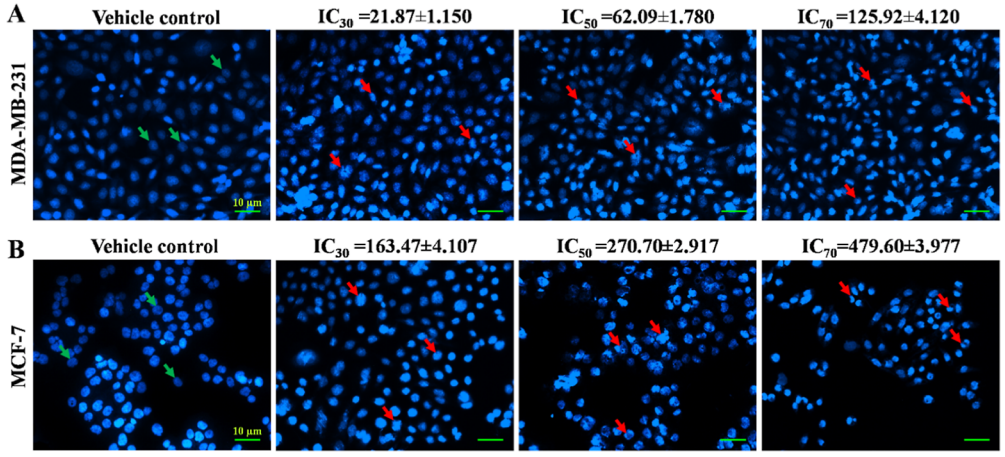

Figure 5. Nuclear morphometric analysis using 4′,6-diamidino-2-phenylindole (DAPI) staining in human breast cancer cells. (A) Morphological changes in the nucleus of MDA-MB-231 cells in the vehicle control group and the EA extract of *C. gloeosporioides* treated group (IC_{30}, IC_{50}, and IC_{70}). (B) Morphological changes in the nucleus of MCF-7 cells in vehicle control and the EA extract of *C. gloeosporioides* treated group (IC_{30}, IC_{50}, and IC_{70}). Scale bar = 10 μm.

gloeosporioides to measure the inhibition of two-dimensional wound closure ability of human breast cancer cells MDA-MB-231 (Figure 4A) and MCF-7 (Figure 4C). In order to evaluate the recovery percentage (% *R*), the area free of migrating cells was determined at 0 h and after 24 h of treatment with the EA extract *C. gloeosporioides* in both vehicle control and treated groups. The recovery percentage (% *R*) in the vehicle control group of both breast cancer cells MDA-MB-231 and MCF-7 was maximum as compared to treated groups, suggesting that the EA extract *C. gloeosporioides* exhibits the potential to inhibit the cancer cell proliferation and migration ability. The recovery percentage (% *R*) induced by the EA extract *C. gloeosporioides* at IC_{30}, IC_{50}, and IC_{70} in MDA-MB-231 cells (Figure 4B) was 31.34 ± 2.428% (*t*-value 9.921; *p*-value 0.001), 12.81 ± 2.675% (*t*-value 17.771; *p*-value 0.000), and 4.49 ± 1.017% (*t*-value 27.878; *p*-value 0.000), respectively, whereas the recovery percentage in the vehicle control group of MDA-MB-231 cells was 52.63 ± 2.812%. Similarly, the MCF-7 cells (Figure 4D) treated with the EA extract of *C. gloeosporioides* at IC_{30}, IC_{50}, and IC_{70} showed the recovery percentage (% *R*) of 38.41 ± 2.645% (*t*-value 19.265; *p*-value 0.000), 29.48 ± 1.272% (*t*-value 31.825; *p*-value 0.000), and 12.02 ± 3.082% (*t*-value 30.100; *p*-value 0.000), respectively. Furthermore, the recovery percentage in the vehicle control group for MCF-7 cells was 34.19 ± 1.220%, and the cell free area is thinner than that of the vehicle control group of MDA-MB-231 cells.

One of the key characteristics of metastatic breast cancer cells is the cell migration and proliferation; therefore, bioactive compounds with the potential to inhibit cancer cell mobility may be critical in the regulation of cancer progression.[48] Such unique ability of bioactive compounds may increase the survival time of the patients of breast cancer. In the present study, wound healing assay indirectly showed the EA extract of *C. gloeosporioides* mediated inhibition of proliferation and migration ability of breast cancer cells. The result revealed that the area created at 0 h by a 20−200 μL pipette tip remained significantly unfilled by migrating cells and cell-free area % after 24 h of treatment with respective IC_{30}, IC_{50}, and IC_{70} of the EA extract *C. gloeosporioides* was 68.66, 87.19, and 95.51% in MDA-MB-231 cells and 61.59, 70.52, and 87.98% in MCF-7 cells, respectively, as compared to the vehicle control group 47.37% (MDA-MB-231) and 26.18% (MCF-7). Serum deprivation leads to cell cycle arrest and thereby inhibits the cell proliferation.[49] Therefore, wound healing assay was performed under low serum (2% fetal bovine serum) condition to validate that the filling of gap is the result of collective migration of MDA-MB-231 and MCF-7 cells, not the proliferation of cells. Accumulating body of evidence suggest that the bioactive compounds of various fungal endophytes possess potential cytotoxic ability, suppression of proliferation, and cell migration of cancer cells including MDA-MB-231 and MCF-7.[50−52] The current study showed that bioactive compounds produced from the endophyte *C. gloeosporioides* significantly inhibited the filling of wound created in MDA-MB-231 and MCF-7 cells. Therefore, the wound healing ability induced by the EA extract of *C. gloeosporioides* indicates that the bioactive compound produced by the endophyte *C. gloeosporioides* may appear to be an effective lead molecule in the treatment of breast cancer.

EA Extract of *C. gloeosporioides* Induces Alteration in Nuclear Morphology in Breast Cancer Cells. In order to get better insight into anticancer mechanism, the cellular and nuclear morphometric changes induced by the EA extract of *C. gloeosporioides* in breast cancer cells, MDA-MB-231 (Figure 5A) and MCF-7 (Figure 5B), were evaluated by 4′,6-diamidino-2-phenylindole (DAPI) staining. The significant reduction in viable cells was observed in both vehicle control group and the EA extract of *C. gloeosporioides* treated group. Staining with DAPI revealed alteration in cellular and nuclear morphology having irregular-shaped nucleus, increased number of nuclear body fragments, and chromatin condensation, indicating apoptosis, whereas the live cells having intact cellular and nuclear morphology with uniformly shaped nucleus without chromatin condensation were observed in the vehicle control group. The alteration in cellular morphology and appearance of irregular nuclear bodies in both MDA-MB-231 and MCF-7 cells was found to be increased with increasing concentration of the EA extract of *C. gloeosporioides*. Overall, the DAPI staining of breast cancer cells MDA-MB-231 and MCF-7 suggest the apoptosis inducing potential of the EA extract of *C. gloeosporioides*.

The outer membrane of cancer cells undergoes a variety of physical alterations during apoptosis, which include a gradual increase in cell membrane porosity that allows the entry of

https://doi.org/10.1021/acsomega.2c05746
ACS Omega 2023, 8, 3768−3784

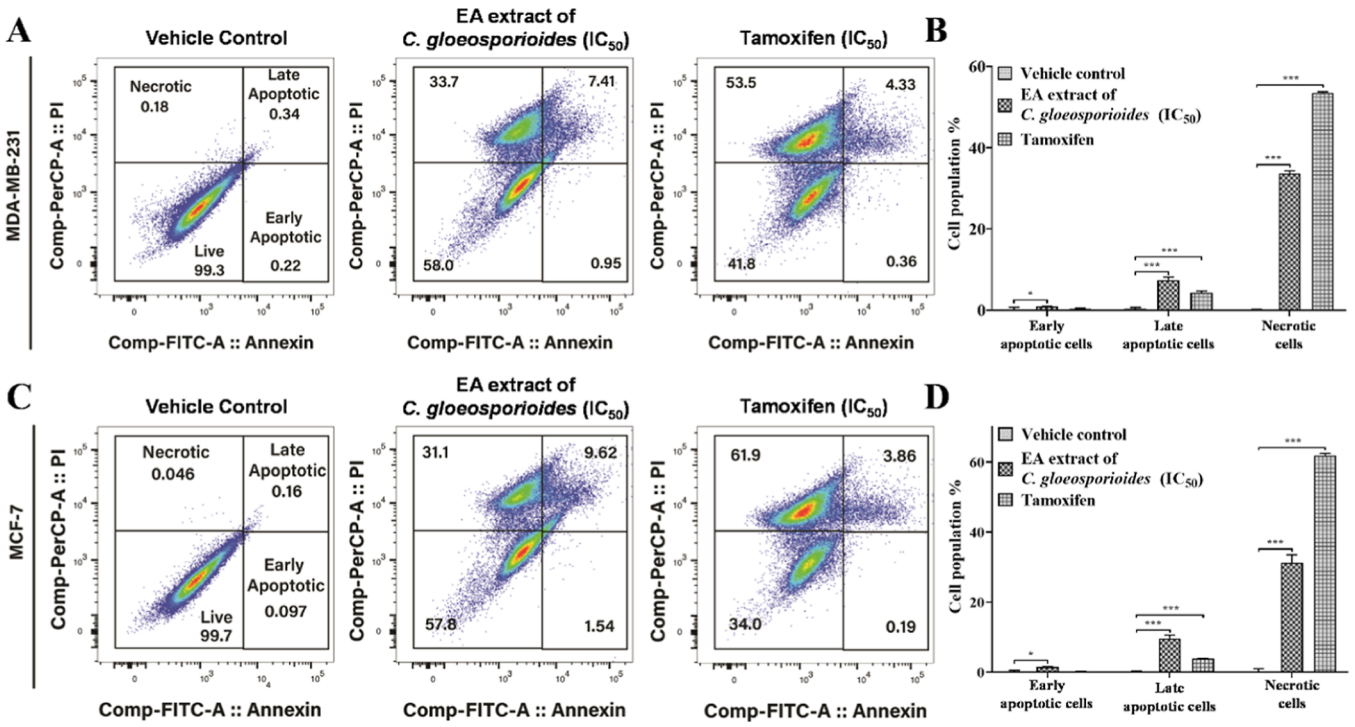

Figure 6. EA extract of *C. gloeosporioides* mediated apoptosis in MDA-MB-231 and MCF-7 cells. (A) Dot plot graph and (B) quantification of early, late, and necrotic cell population in MDA-MB-231 cells treated with the EA extract of *C. gloeosporioides* and tamoxifen as compared to vehicle control. (C) Dot plot graph and (D) quantification of early, late, and necrotic cell population in MCF-7 cells treated with the EA extract of *C. gloeosporioides* and tamoxifen with respect to vehicle control. *p*-value was calculated using one-way ANOVA, followed by Tukey's test to compare the mean ± SD of percentage of cell population in early, late, and necrotic stages treated with the EA extract of *C. gloeosporioides* and tamoxifen with vehicle control. The statistical significance is as follows: ***, $p \leq 0.001$; **, $p \leq 0.002$; and *, $p \leq 0.033$.

prominent staining dyes such as DAPI. DAPI enters into MDA-MB-231 and MCF-7 cells treated with the EA extract of *C. gloeosporioides* and binds strongly with adenine−thymine (A−T)-rich regions giving a bright blue color.[53] A previous study also validates our result by suggesting that the EA extract of fungal endophytes and natural bioactive compounds has the ability to induce nuclear fragmentation and condensation, reduction in cell size, and appearance of dispersed apoptotic bodies in breast cancer cells.[51,54,55] Taken together, the study revealed that the EA extract of *C. gloeosporioides* causes alteration in cellular and nuclear morphologies in both cancer cells, MDA-MB-231 and MCF-7, and thereby leads to apoptosis. Further, the quantitative assessment of apoptosis-inducing potential of the EA extract of *C. gloeosporioides* was shown through Annexin V-FITC/PI double staining.

EA Extract of *C. gloeosporioides* Induces Apoptosis in Breast Cancer Cells. The apoptosis-inducing potential of the EA extract of *C. gloeosporioides* in breast cancer cells was studied through flow cytometry analysis using Annexin V-FITC and PI dual staining. The extent of apoptosis in MDA-MB-231 and MCF-7 cells induced by the EA extract of *C. gloeosporioides* was elucidated by analyzing the percentage of early apoptotic, late apoptotic, and necrotic cell population, which was further compared with Tamoxifen. Dot-plot graphs demonstrated that the distribution of MDA-MB-231 (Figure 6A) and MCF-7 (Figure 6C) cells in four cellular events such as live (lower left quadrant), early phase of apoptosis (lower right quadrant), late phase of apoptosis (upper right quadrant), and necrotic (upper left quadrant). The result showed that the EA extract of *C. gloeosporioides* and tamoxifen (standard drug) potentially induces the apoptosis rate in MDA-MB-231 (Figure 6B) and MCF-7 (Figure 6D) cells as compared to vehicle control. Treatment with the EA extract of *C. gloeosporioides* for 24 h led to increase the early apoptotic MDA-MB-231 cells to 0.95 ± 0.035% (*p*-value 0.047) and late apoptotic cells to 7.41 ± 0.707% (*p*-value 0.000) as compared to the vehicle control group 0.22 ± 0.502 and 0.34 ± 0.339%, respectively, whereas the percentage of necrotic cell was increased to 33.7 ± 0.636% (*p*-value 0.000) as compared to the vehicle control group 0.18 ± 0.042%. Upon treatment with tamoxifen, the population of MDA-MB-231 cells in early apoptotic, late apoptotic, and necrotic phase cells were 0.36 ± 0.167% (*p*-value 0.806), 4.33 ± 0.381% (*p*-value 0.000), and 53.5 ± 0.283% (*p*-value 0.000) as compared to vehicle control. Similarly, treatment with the EA extract of *C. gloeosporioides* led to increase the early apoptotic MCF-7 cells to 1.54 ± 0.057% (*p*-value 0.000), late apoptotic cells to 9.62 ± 0.983% (*p*-value 0.000), and necrotic cells to 31.3 ± 2.263% (*p*-value 0.000) as compared to the vehicle control group to 0.10 ± 0.453, 0.16 ± 0.170, and 0.05 ± 0.940%, respectively, whereas the percentages of population of tamoxifen-treated MCF-7 cells in early apoptotic, late apoptotic, and necrotic phase cell were 0.19 ± 0.035% (*p*-value 0.884), 3.86 ± 0.077% (*p*-value 0.000), and 61.9 ± 0.566% (*p*-value 0.000) as compared to vehicle control.

One of the most reliable methods for the quantitative assessment for the detection of live, early, late apoptosis or in necrotic stage is dual staining with FITC-labeled Annexin V (Annexin V-FITC) and PI. The first sign of apoptosis is the loss of asymmetry in the plasma membrane. The initiation of the EA extract of *C. gloeosporioides* induced apoptosis in MDA-MB-231 and MCF-7 was validated by Annexin V-FITC/PI staining. The inner leaflet of healthy cells normally contains

https://doi.org/10.1021/acsomega.2c05746
ACS Omega 2023, 8, 3768−3784

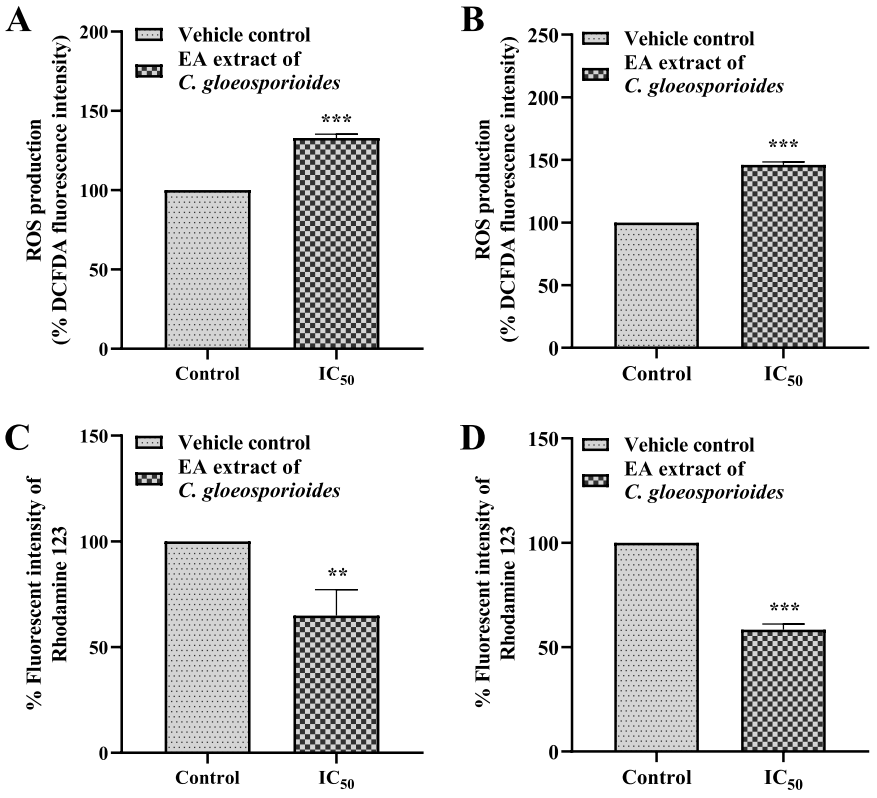

Figure 7. EA extract of *C. gloeosporioides* induces the generation ROS in (A) MDA-MB-231 and (B) MCF-7 cells and diminishes the MMP in (C) MDA-MB-231 and (D) MCF-7 cells. Data are represented as the mean ± SD of the EA extract of *C. gloeosporioides* treated group as compared to vehicle control. The statistical significance (***, $p < 0.001$; **, $p < 0.010$; and *, $p < 0.050$) was calculated by performing independent Student's *t*-test.

phosphatidylserine (PS), an anionic phospholipid. Nevertheless, during apoptosis, the PS is transferred to the outer leaflet. In flow cytometry analysis, fluorescein isothiocyanate-labeled Annexin V (Annexin V-FITC) and PI bind with PS and thus differentiate between live (healthy) cells and apoptotic or necrotic cells. Both stains are negative for normal cells, and the early apoptotic cells are positive for Annexin V-FITC only, while late apoptotic cells are positive for both Annexin V-FITC and PI stains. The observation showed weak staining of cell membrane in live cells with Annexin V, whereas higher degree of surface labeling was observed for apoptotic cells as there is no externalization of PS and thus no apoptotic signal in live or healthy cells.[56] The treatment with the EA extract of *C. gloeosporioides* showed a decrease in the level of live cells (Annexin V^-/PI^-), while a significant increase in early (Annexin V^+/PI^-), late (Annexin V^+/PI^+), apoptotic, and necrotic (Annexin V^-/PI^+) cells, thus evidencing its apoptosis inducing potential against MDA-MB-231 and MCF-7 cells. Previous studies have also demonstrated similar findings using marine algal-derived endophytic fungus *Aspergillus* sp. and apoptotic events in HeLa cells after treatment with fungal extract was evidenced using Annexin V-FITC/PI staining.[57] A study performed using Annexin V-FITC and PI dual staining also showed that the fungal endophyte *Cladosporium cladosporioides* derived bioactive compound cladosporol A significantly induces apoptosis in MCF-7 cells.[55]

EA Extract of *C. gloeosporioides* Induces ROS Production and Depolarizes the Mitochondrial Membrane Potential in Breast Cancer Cells. We further investigated the involvement of the ROS-dependent signal transduction pathway in the induction of apoptosis by the EA extract of *C. gloeosporioides* in MDA-MB-231 and MCF-7 cells using the DCFH-DA dye method. Our results showed that treatment with IC_{50} of the EA extract of *C. gloeosporioides* to MDA-MB-231 cells causes the increased production of ROS by 132.89 ± 2.407% (*t*-value −23.662; *p*-value 0.000) as compared to the vehicle control group (Figure 7A), whereas MCF-7 cells treated with the IC_{50} values of the EA extract of *C. gloeosporioides* led to the increased generation of ROS by 146.11 ± 2.208% (*t*-value −36.177; *p*-value 0.000) (Figure 7B) as compared to the vehicle control group. Since the generation of ROS is highly related with the impaired MMP, therefore, we further investigated the level of MMP in the EA extract of *C. gloeosporioides* treated breast cancer cells. Our results showed that the level of MMP was mitigated by 64.87 ± 12.331% (*t*-value 4.934; *p*-value 0.008) (Figure 7C) in MDA-MB-231 cells after treatment with the EA extract of *C. gloeosporioides* as compared to the vehicle control group. Similarly, in MCF-7 cells, the level of MMP was also decreased to 58.32 ± 2.798% (*t*-value 25.806; *p*-value 0.000) (Figure 7D) upon treatment with the EA extract of *C. gloeosporioides* as compared to vehicle control.

Mitochondria play a critical role in the apoptosis of cancer cells under the influence of drug. According to a number of scientific studies, disruption in MMP is a hallmark of early apoptosis.[58,59] ROS is essential for many cellular biological functions, including the cancer metastasis and progression. During earlier studies, it has been anticipated that targeting ROS is a critically significant approach for cancer therapeutics. Paclitaxel, a remarkable anticancer drug, is known to induce apoptosis in cancer by elevating the production of ROS. Thus, the bioactive compounds which induce the increased

https://doi.org/10.1021/acsomega.2c05746
ACS Omega 2023, 8, 3768−3784

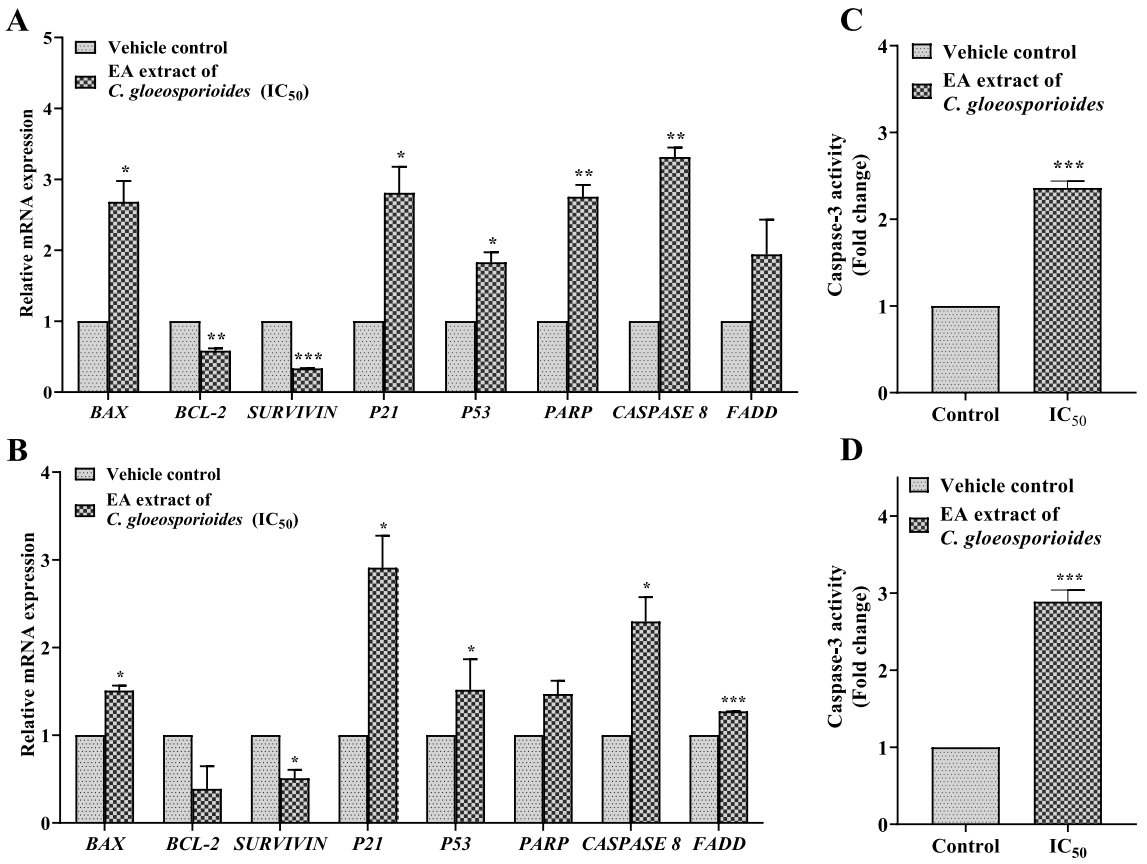

Figure 8. qRT-PCR analysis showing differential mRNA expression of genes associated with pro-apoptosis (*BAX*, *PARP*, *CASPASE-8*, and *FADD*), antiapoptosis (*BCL-2* and *SURVIVIN*), cell cycle arrest (*P21*), and tumor suppression (*P53*). Histogram represents the fold change in relative gene expression in (A) MDA-MB-231 and (B) MCF-7 cells with respect to vehicle control. *In vitro* expression level of the active form of caspase-3 in the EA extract of *C. gloeosporioides* (IC_{50}) treated (C) MDA-MB-231 and (D) MCF-7 cells as compared to vehicle control. The statistical significance (***, $p < 0.001$; **, $p < 0.010$; and *, $p < 0.050$) was calculated by performing independent Student's *t*-test.

production of ROS are thought to be a potential molecule for cancer therapeutics.[60] The study showed that the bioactive compound cladosporol A isolated from the endophytic fungus *C. cladosporioides* induces apoptosis in MCF-7 cells by increased production of ROS and decreased level of MMP.[55] Additionally, various inhibitors such as the PDGFR inhibitor (imatinib), tyrosine kinase inhibitors, and EGFR inhibitor (erlotinib) are used as a therapeutic approach toward cancer cells that follows ROS-dependent apoptosis through depolarization of MMP.[61,62] Therefore, we assessed the involvement of the role of mitochondria in the EA extract of *C. gloeosporioides* induced apoptosis in the human breast cancer cells MDA-MB-231 and MCF-7. We observed that the EA extract of *C. gloeosporioides* decreased the level of ΔΨm in MDA-MB-2321 and MCF-7 cells. Our findings, which are in line with earlier research, support the notion that the EA extract of *C. gloeosporioides* induces ROS generation and depolarization of MMP that may lead to the apoptosis of breast cancer cells.

EA Extract of *C. gloeosporioides* Induces Differential Gene Expression of Apoptosis, Cell Cycle Arrest, and Tumor Suppressor-Related Genes in Breast Cancer Cells. The EA extract of *C. gloeosporioides* induced antiproliferative mechanism in human breast cancer cells was shown through relative gene expressions using q-RT-PCR analysis. The fold change in the expression of apoptosis (*BAX*, *BCL-2*, *SURVIVIN*, *PARP*, *CASPASE-8*, and *FADD*), cell cycle arrest (*P21*), and tumor suppressor (*P53*)-related genes in vehicle control was considered as 1 and compared with MDA-MB-231 (Figure 8A) and MCF-7 (Figure 8B) cells treated with the IC_{50} value of the EA extract of *C. gloeosporioides*. The relative mRNA expression of pro-apoptotic gene *BAX* was significantly increased to 2.68 ± 0.296-fold (*t*-value −5.682; *p*-value 0.030) and 1.51 ± 0.059 fold (*t*-value −8.675; *p*-value 0.013) in MDA-MB-231 and MCF-7 cells, respectively, whereas the expression of antiapoptotic genes such as *BCL-2* and *SURVIVIN* was decreased by 0.58 ± 0.035-fold (*t*-value 11.943; *p*-value 0.007) and 0.33 ± 0.006-fold (*t*-value 111.167; *p*-value 0.000) and 0.39 ± 0.260-fold (*t*-value 2.358; *p*-value 0.142) and 0.51 ± 0.097 fold (*t*-value 5.072; *p*-value 0.037) in MDA-MB-231 and MCF-7 cells, respectively. Furthermore, the expression of gene responsible for cell cycle inhibition *P21* was significantly increased to 3.06 ± 0.618 fold (*t*-value −4.908; *p*-value 0.039) in MDA-MB-231 and 2.91 ± 0.367 fold (*t*-value −5.199; *p*-value 0.035) in MCF-7 cells. Besides, the relative mRNA expression level of tumor suppressor gene (*P53*) was significantly increased by 1.83 ± 0.141-fold (*t*-value −5.887; *p*-value 0.028) and 1.52 ± 0.351 (*t*-value −4.723; *p*-value 0.042) fold in MDA-MB-231 and MCF-7 cells, respectively. Besides these genes, we have also evaluated the differential expression of genes associated with an extrinsic pathway including *CASPASE-8*, *PARP*, and *FADD*. The results showed that the relative expression of mRNA of the pro-apoptotic gene *PARP* was significantly increased by 2.75 ± 0.169-fold (*t*-value

https://doi.org/10.1021/acsomega.2c05746
ACS Omega 2023, 8, 3768−3784

−10.373; *p*-value 0.009) and 1.47 ± 0.154-fold (*t*-value −3.026; *p*-value 0.094) in MDA-MB-231 and MCF-7 cells, respectively, whereas the relative expression of pro-apoptotic genes such as *CASPASE-8* and *FADD* was upregulated by 3.31 ± 0.136-fold (*t*-value −17.007; *p*-value 0.003) and 1.94 ± 0.492-fold (*t*-value −1.911; *p*-value 0.196) and 2.30 ± 0.279-fold (*t*-value −4.642; *p*-value 0.043) and 1.27 ± 0.002-fold (*t*-value −135.00; *p*-value 0.000) in MDA-MB-231 and MCF-7 cells, respectively.

Considering the increased level of ROS and decreased level of MMP, the differential expression of genes related to intrinsic as well as extrinsic pathways was evaluated in MDA-MB-231 and MCF-7 cells treated with the EA extract of *C. gloeosporioides*. The results showed that the EA extract of *C. gloeosporioides* induces the differential expression of genes associated with the intrinsic as well as extrinsic pathways in both breast cancer cells. The increased ROS level can significantly endorse the expression of *P53*. Bax, the primary inducer of the mitochondrial mediated intrinsic apoptotic pathway, is a proapoptotic factor that belongs to the Bcl-2 protein family[63] since Bcl-2 suppresses the release of cytochrome-c from the mitochondria and blockage of caspase activation, which are the signal molecule for apoptotic induction. Our results showed that treatment with the EA extract of *C. gloeosporioides* causes a decrease in the expression of *BCL-2* gene, suggesting that the activation of Bax and other pro-apoptotic factors leads to the apoptosis of breast cancer cells. Further, the increased expression of *P21* and *P53* gene suggests that the EA extract of *C. gloeosporioides* induces cell cycle inhibition and tumor suppression in breast cancer cells. According to previous findings, p53 causes a conformational change in amino terminus that directs the release of cytochrome *c* from depolarized mitochondria and subsequently triggered the intrinsic apoptotic pathway mediated by mitochondria.[64,65] Besides, the EA extract of *C. gloeosporioides* induces apoptosis by the extrinsic pathways following the activation of *FADD*, *CASPASE-8*, and *PARP*. Conclusively, our finding suggest that the bioactive compounds produced from the endophyte *C. gloeosporioides* induced apoptosis may be by following both intrinsic and extrinsic pathways in human breast cancer cells.

EA Extract of *C. gloeosporioides* Induces Apoptosis via the Mitochondria-Mediated Apoptotic Pathway in Breast Cancer Cells. After observing the tumor growth inhibitory action of the EA extract of *C. gloeosporioides* in breast cancer cells MDA-MB-231 and MCF-7, we further studied the apoptosis pathway induced by the EA extract of *C. gloeosporioides*. The ability of the EA extract of *C. gloeosporioides* to induce apoptosis in MDA-MB-231 and MCF-7 cells was confirmed by immunoblotting by analyzing the expression levels of the apoptosis regulating protein Bcl-2. Additionally, the effect of the EA extract of *C. gloeosporioides* was also evaluated on the activity of the active form of caspase-3 in MDA-MB-231 and MCF-7 cells. Notably, our results showed that the EA extract of *C. gloeosporioides* markedly inhibited the expression level of Bcl-2 (an antiapoptotic protein) in both breast cancer cells as compared to the respective vehicle control (Figure S2A,B). The EA extract of *C. gloeosporioides* significantly upregulated the expression level of the active form of Caspase-3 by 2.35 ± 0.296 fold (*t*-value −29.55; *p*-value 0.000) in MDA-MB-231 (Figure 8C), as compared to their controls. Similarly, the expression of the active form of Caspase-3 was also found to be elevated by 2.86 ± 0.219 fold (*t*-value −21.57; *p*-value 0.000) in MCF-7 cells (Figure 8D) upon treatment with the EA extract of *C. gloeosporioides*. Taken together, our findings suggested that the EA extract of *C. gloeosporioides* attenuates the proliferation of human breast cancer cells by inducing apoptosis. The cytotoxic activity of the EA extract of *C. gloeosporioides* has been previously reported in cancer of different origins like colorectal, liver, and breast.[23] Induction of apoptosis is considered as one of the important properties of an anticancer drug.[66] Hence, to investigate the anticancer therapeutic potential of the EA extract of *C. gloeosporioides* against breast cancer, we evaluated the apoptosis inducing ability of the EA extract of *C. gloeosporioides* by examining the expression levels of an antiapoptotic protein Bcl-2. Additionally, the EA extract of *C. gloeosporioides* also induces the expression of the active form of Caspapse-3 in human breast cancer cells, MDA-MB-231 and MCF-7. One important signaling mechanism that induces cancer cell death is the mitochondrial pathway. The Bcl-2 family protein plays a significant role in apoptosis induced by the mitochondrial mediated pathway.

The drug or bioactive compounds that cause apoptosis may activate apoptosis-related factors that further lead to the activation of pro-apoptotic proteins Bax, the active form of Caspapse-3, and downregulate the antiapoptotic proteins including Bcl-2. Furthermore, these Bcl-2 family proteins could be transported to the outer mitochondrial membrane and alter the permeability of the mitochondrial membrane and depolarize the MMP, thereby enabling the mitochondria to release apoptosis inducing factors. Interestingly, our results also showed the decreased level of antiapoptotic protein Bcl-2 while increased expression of the active form of Caspase-3 in the EA extract of *C. gloeosporioides* treated human breast cancer cells MDA-MB-231 (Figure 8C) and MCF-7 (Figure 8D). Studies also suggest that the increased generation of ROS may induce the apoptotic process in cancer cells by modulating the expression level of pro-apoptotic and antiapoptotic proteins. ROS induces the apoptosis by downregulating the expression of crucial antiapoptotic protein Bcl-2 by increasing the ubiquitination.[67] Our findings, which are in line with earlier research, support the notion that the EA extract of *C. gloeosporioides* induces ROS generation, leading to apoptosis in human breast cancer cells. Overall, our findings demonstrate that the fungal endophyte *C. gloeosporioides* produces bioactive compounds with potential anticancer activity, which induces mitochondria-mediated apoptosis in MDA-MB-231 and MCF-7 cells, further suggesting that the fungal endophyte *C. gloeosporioides* could be a potential therapeutic target for the discovery of novel drugs against breast cancer.

CONCLUSIONS

Fungal endophytes are a remarkable repertoire of bioactive compounds which can be used as budding sources of pharmaceutical lead compounds in drug discovery and development against breast cancer. The current study showed that the EA extract of *C. gloeosporioides* exhibited potential cytotoxic activity against human breast cancer cells MDA-MB-231 and MCF-7 but not against non-cancerous HEK293T cells. The reduction in the number of colonies and the decreased expression of *CD44* gene suggest that the bioactive compounds produced by *C. gloeosporioides* has the potential to inhibit the stemness characteristics such as self-renewal, proliferation, and differentiation of both breast cancer cells. Furthermore, the EA extract of *C. gloeosporioides* promotes the

https://doi.org/10.1021/acsomega.2c05746
ACS Omega 2023, 8, 3768−3784

alteration in cellular and nuclear morphologies and inhibits the proliferation and migration of breast cancer cells, MDA-MB-231 and MCF-7. Moreover, Annexin V-FITC/PI staining of both breast cancer cells treated with the EA extract of *C. gloeosporioides* validates its apoptosis inducing potential. The EA extract of *C. gloeosporioides* causes increases in the production of ROS and depolarization of the MMP, thereby potentiating apoptosis in both breast cancer cells. Additionally, the bioactive compounds present in the EA extract of *C. gloeosporioides* induces apoptosis in MDA-MB-231 and MCF-7 cells by promoting the differential expression of pro-apoptotic and antiapoptotic genes and the active form of Caspase-3. Overall, our result suggests that the bioactive compounds present in the EA extract of *C. gloeosporioides* could be an efficient anticancer agent in the treatment of human breast cancer. However, further research work is intended to elucidate the in vivo anticancer activity on breast cancer model to validate the mechanistic action of the EA extract of *C. gloeosporioides*.

■ ASSOCIATED CONTENT

Supporting Information

The Supporting Information is available free of charge at https://pubs.acs.org/doi/10.1021/acsomega.2c05746.

List of primers; list of bioactive compounds identified through GC/MS analysis of the EA extract of the fungal endophyte *C. gloeosporioides*; qRT-PCR analysis showing differential mRNA expression of *CD44* gene; and immunoblot for the expression of antiapoptotic protein Bcl-2 (PDF)

■ AUTHOR INFORMATION

Corresponding Author

Vibhav Gautam − *Centre of Experimental Medicine and Surgery, Institute of Medical Sciences, Banaras Hindu University, Varanasi 221005, India;* orcid.org/0000-0001-7956-9555; Phone: +918860182113; Email: vibhav.gautam4@bhu.ac.in, vibhavgautam16@gmail.com

Authors

Nilesh Rai − *Centre of Experimental Medicine and Surgery, Institute of Medical Sciences, Banaras Hindu University, Varanasi 221005, India*

Priyamvada Gupta − *Centre of Experimental Medicine and Surgery, Institute of Medical Sciences, Banaras Hindu University, Varanasi 221005, India*

Ashish Verma − *Centre of Experimental Medicine and Surgery, Institute of Medical Sciences, Banaras Hindu University, Varanasi 221005, India*

Rajan Kumar Tiwari − *Department of Zoology, Institute of Science, Banaras Hindu University, Varanasi 221005, India*

Prasoon Madhukar − *Infectious Disease Research Laboratory, Department of Medicine, Institute of Medical Sciences, Banaras Hindu University, Varanasi 221005, India*

Swapnil C. Kamble − *Department of Technology, Savitribai Phule Pune University, Pune 411007, India;* orcid.org/0000-0002-7501-2044

Ajay Kumar − *Department of Zoology, Institute of Science, Banaras Hindu University, Varanasi 221005, India*

Rajiv Kumar − *Centre of Experimental Medicine and Surgery, Institute of Medical Sciences, Banaras Hindu University, Varanasi 221005, India*

Santosh Kumar Singh − *Centre of Experimental Medicine and Surgery, Institute of Medical Sciences, Banaras Hindu University, Varanasi 221005, India*

Complete contact information is available at: https://pubs.acs.org/10.1021/acsomega.2c05746

Author Contributions

N.R. contributed to data curation, formal analysis, investigation, methodology, roles/writing—original draft, software, writing—review and editing, and visualization. P.G. contributed to data curation, formal analysis, investigation, and writing—review and editing. A.V. contributed to data curation, formal analysis, investigation, and writing—review and editing. R.K.T. contributed to data curation and writing—review and editing. P.M. contributed to writing—review and editing. S.K. contributed to data curation and writing—review and editing. A.K. contributed to data curation and writing—review and editing. R.K. contributed to writing—review and editing. S.K.S. contributed to writing—review and editing. V.G. contributed to conceptualization, methodology, formal analysis, funding acquisition, investigation, project administration, resources, software, and writing—review and editing.

Notes

The authors declare no competing financial interest.

■ ACKNOWLEDGMENTS

N.R. would like to thank University Grants Commission, New Delhi, India, for Junior and Senior Research Fellowship. P.G. would like to thank SERB India for Junior Research Fellowship under Empowerment and Equity Opportunities for Excellence in Science (EMEQ) scheme. A.V. would like to thank the Council of Scientific and Industrial Research, New Delhi, India, for Junior Research Fellowship. This work was supported by the Science and Engineering Research Board (SERB)-EMEQ grant (EEQ/2019/000025) to V.G. V.G. also acknowledges the funding support to his lab from the Institution of Eminence Seed Grant, Banaras Hindu University, Varanasi, India. R.K. acknowledges the internal funding from Banaras Hindu University, Varanasi, India (under the Institute of Eminence Scheme). The corresponding author on behalf of all the author acknowledges the Interdisciplinary School of Life Sciences (ISLS), Banaras Hindu University, Varanasi, India, for the fluorescence microscopy facility and the Sophisticated Analytical Instrumentation Facility (SAIF), Panjab University, India, for the GC/MS facility. We sincerely acknowledge Dr. S. B. Chauhan (IDRL, IMS-BHU, India) for helping in Flow Cytometry experiments.

■ REFERENCES

(1) Hyde, K. D.; Soytong, K. The fungal endophyte dilemma. *Fungal Diversity* **2008**, *33*, No. e173.

(2) Rai, N.; Kumari Keshri, P.; Verma, A.; Kamble, S. C.; Mishra, P.; Barik, S.; Kumar Singh, S.; Gautam, V. Plant associated fungal endophytes as a source of natural bioactive compounds. *Mycology* **2021**, *12*, 139−159.

(3) Atri, N.; Rai, N.; Singh, A. K.; Verma, M.; Barik, S.; Gautam, V.; Singh, S. K. Screening for endophytic fungi with antibacterial efficiency from Moringa oleifera and Withania somnifera. *J. Sci. Res.* **2020**, *64*, 127−133.

(4) Oberhofer, M.; Wackerlig, J.; Zehl, M.; Büyük, H.; Cao, J. J.; Prado-Roller, A.; Urban, E.; Zotchev, S. B. Endophytic Akanthomyces sp. LN303 from Edelweiss produces emestrin and two new 2-hydroxy-4 pyridone alkaloids. *ACS Omega* **2021**, *6*, 2184−2191.
(5) Gupta, P.; Verma, A.; Rai, N.; Singh, A. K.; Singh, S. K.; Kumar, B.; Kumar, R.; Gautam, V. Mass Spectrometry-Based Technology and Workflows for Studying the Chemistry of Fungal Endophyte Derived Bioactive Compounds. *ACS Chem. Biol.* **2021**, *16*, 2068−2086.
(6) Wei, J.; Chen, F.; Liu, Y.; Abudoukerimu, A.; Zheng, Q.; Zhang, X.; Sun, Y.; Yimiti, D. Comparative Metabolomics Revealed the Potential Antitumor Characteristics of Four Endophytic Fungi of Brassica rapa L. *ACS Omega* **2020**, *5*, 5939−5950.
(7) Salvi, P.; Kumar, G.; Gandass, N.; Kajal, A.; Verma, S.; Rajarammohan, N.; Rai, V.; Gautam, V. Antimicrobial Potential of Essential Oils from Aromatic Plant Ocimum sp.; A Comparative Biochemical Profiling and In-Silico Analysis. *Agronomy* **2022**, *12*, 627.
(8) Barik, S.; Rai, N.; Mishra, P.; Singh, S. K.; Gautam, V. Bioinformatics: How it helps to boost modern biological research. *Curr. Sci.* **2020**, *118*, 698−699.
(9) Salvi, P.; Mahawar, H.; Agarrwal, R.; Kajal; Gautam, V.; Deshmukh, R. Advancement in the molecular perspective of plant-endophytic interaction to mitigate drought stress in plants. *Front. Microbiol.* **2022**, *13*, 981355.
(10) Rodriguez, R.; Redman, R. More than 400 million years of evolution and some plants still can't make it on their own: plant stress tolerance via fungal symbiosis. *J. Exp. Bot.* **2008**, *59*, 1109−1114.
(11) Card, S.; Johnson, L.; Teasdale, S.; Caradus, J. Deciphering endophyte behaviour: the link between endophyte biology and efficacious biological control agents. *FEMS Microbiol. Ecol.* **2016**, *92*, fiw114.
(12) Tan, R. X.; Zou, W. X. Endophytes: a rich source of functional metabolites (1987 to 2000). *Nat. Prod. Rep.* **2001**, *18*, 448−459.
(13) Gunatilaka, A. L. Natural products from plant-associated microorganisms: distribution, structural diversity, bioactivity, and implications of their occurrence. *J. Nat. Prod.* **2006**, *69*, 509−526.
(14) Tawfike, A. F.; Romli, M.; Clements, C.; Abbott, G.; Young, L.; Schumacher, M.; Diederich, M.; Farag, M.; Edrada-Ebel, R. Isolation of anticancer and anti-trypanosome secondary metabolites from the endophytic fungus Aspergillus flocculus via bioactivity guided isolation and MS based metabolomics. *J. Chromatogr. B: Anal. Technol. Biomed. Life Sci.* **2019**, *1106-1107*, 71−83.
(15) Creamer, R.; Hille, D. B.; Neyaz, M.; Nusayr, T.; Schardl, C. L.; Cook, D. Genetic Relationships in the Toxin-Producing Fungal Endophyte, Alternaria oxytropis Using Polyketide Synthase and Non-Ribosomal Peptide Synthase Genes. *J. Fungi* **2021**, *7*, 538.
(16) Keshri, P. K.; Rai, N.; Verma, A.; Kamble, S. C.; Barik, S.; Mishra, P.; Singh, S. K.; Salvi, P.; Gautam, V. Biological potential of bioactive metabolites derived from fungal endophytes associated with medicinal plants. *Mycol. Prog.* **2021**, *20*, 577−594.
(17) Ranjan, A.; Singh, R. K.; Khare, S.; Tripathi, R.; Pandey, R. K.; Singh, A. K.; Gautam, V.; Tripathi, J. S.; Singh, S. K. Characterization and evaluation of mycosterol secreted from endophytic strain of Gymnema sylvestre for inhibition of α-glucosidase activity. *Sci. Rep.* **2019**, *9*, 17302.
(18) Zou, W.; Meng, J.; Lu, H.; Chen, G.; Shi, G.; Zhang, T.; Tan, R. Metabolites of Colletotrichum gloeosporioides, an endophytic fungus in Artemisia mongolica. *J. Nat. Prod.* **2000**, *63*, 1529−1530.
(19) Meyer, W. L.; Lax, A. R.; Templeton, G. E.; Brannon, M. J. The structure of gloeosporone, a novel germination self-inhibitor from conidia of Collectotrichum gloeosporioides. *Tetrahedron Lett.* **1983**, *24*, 5059−5062.
(20) Ohra, J.; Morita, K.; Tsujino, Y.; Tazaki, H.; Fujimori, T.; Goering, M.; Evans, S.; Zorner, P. Production of the phytotoxic metabolite, ferricrocin, by the fungus Colletotrichum gloeosporioides. *Biosci., Biotechnol., Biochem.* **1995**, *59*, 113−114.
(21) Jagetia, G. C. A review on the medicinal and pharmacological properties of traditional ethnomedicinal plant sonapatha, oroxylum indicum. *Sinusitis* **2021**, *5*, 71−89.
(22) Lalrinzuali, K.; Vabeiryureilai, M.; Jagetia, G. C. Topical application of stem bark ethanol extract of Sonapatha, Oroxylum indicum (L.) Kurz accelerates healing of deep dermal excision wound in Swiss albino mice. *J. Ethnopharmacol.* **2018**, *227*, 290−299.
(23) Rai, N.; Keshri, P. K.; Gupta, P.; Verma, A.; Kamble, S. C.; Singh, S. K.; Gautam, V. Bioprospecting of fungal endophytes from Oroxylum indicum (L.) Kurz with antioxidant and cytotoxic activity. *PLoS One* **2022**, *17*, No. e0264673.
(24) Dhayanithy, G.; Subban, K.; Chelliah, J. Diversity and biological activities of endophytic fungi associated with Catharanthus roseus. *BMC Microbiol.* **2019**, *19*, 22.
(25) Golla, U.; Bhimathati, S. S. R. Evaluation of antioxidant and DNA damage protection activity of the hydroalcoholic extract of Desmostachya bipinnata L. Stapf. *ScientificWorldJournal* **2014**, *2014*, 215084.
(26) Gupta, P.; Rai, N.; Verma, A.; Saikia, D.; Singh, S. P.; Kumar, R.; Singh, S. K.; Kumar, D.; Gautam, V. Green-Based Approach to Synthesize Silver Nanoparticles Using the Fungal Endophyte Penicillium oxalicum and Their Antimicrobial, Antioxidant, and In Vitro Anticancer Potential. *ACS Omega* **2022**, *7*, 46653.
(27) Franken, N. A.; Rodermond, H. M.; Stap, J.; Haveman, J.; van Bree, C. Clonogenic assay of cells in vitro. *Nat. Protoc.* **2006**, *1*, 2315−2319.
(28) Liang, C.-C.; Park, A. Y.; Guan, J.-L. In vitro scratch assay: a convenient and inexpensive method for analysis of cell migration in vitro. *Nat. Protoc.* **2007**, *2*, 329−333.
(29) Shi, J.; Li, J.; Li, J.; Li, R.; Wu, X.; Gao, F.; Zou, L.; Mak, W. W. S.; Fu, C.; Zhang, J.; Leung, G. P.-H. Synergistic breast cancer suppression efficacy of doxorubicin by combination with glycyrrhetinic acid as an angiogenesis inhibitor. *Phytomedicine* **2021**, *81*, 153408.
(30) Rashmi, K.; Harsha Raj, M. H.; Paul, M.; Girish, K. S.; Salimath, B. P.; Aparna, H. A new pyrrole based small molecule from Tinospora cordifolia induces apoptosis in MDA-MB-231 breast cancer cells via ROS mediated mitochondrial damage and restoration of p53 activity. *Chem.-Biol. Interact.* **2019**, *299*, 120−130.
(31) Ronot, X.; Benel, L.; Adolphe, M.; Mounolou, J. Mitochondrial analysis in living cells: the use of rhodamine 123 and flow cytometry. *Biol. Cell* **1986**, *57*, 1−7.
(32) Berman, S. B.; Hastings, T. G. Dopamine oxidation alters mitochondrial respiration and induces permeability transition in brain mitochondria: implications for Parkinson's disease. *J. Neurochem.* **1999**, *73*, 1127−1137.
(33) Gautam, V.; Singh, A.; Yadav, S.; Singh, S.; Kumar, P.; Sarkar Das, S.; Sarkar, A. K. Conserved LBL1-ta-siRNA and miR165/166-RLD1/2 modules regulate root development in maize. *Development* **2021**, *148*, dev190033.
(34) Mishra, E.; Thakur, M. K. Alterations in hippocampal mitochondrial dynamics are associated with neurodegeneration and recognition memory decline in old male mice. *Biogerontology* **2022**, *23*, 251−271.
(35) Jaiswara, P. K.; Gupta, V. K.; Sonker, P.; Rawat, S. G.; Tiwari, R. K.; Pathak, C.; Kumar, S.; Kumar, A. Nimbolide induces cell death in T lymphoma cells: Implication of altered apoptosis and glucose metabolism. *Environ. Toxicol.* **2021**, *36*, 628.
(36) Bradford, M. M. A rapid and sensitive method for the quantitation of microgram quantities of protein utilizing the principle of protein-dye binding. *Anal. Biochem.* **1976**, *72*, 248−254.
(37) Chithra, S.; Jasim, B.; Sachidanandan, P.; Jyothis, M.; Radhakrishnan, E. Piperine production by endophytic fungus Colletotrichum gloeosporioides isolated from Piper nigrum. *Phytomedicine* **2014**, *21*, 534−540.
(38) Manayi, A.; Nabavi, S. M.; Setzer, W. N.; Jafari, S. Piperine as a potential anti-cancer agent: a review on preclinical studies. *Curr. Med. Chem.* **2018**, *25*, 4918−4928.
(39) Baron, J. A.; Sandler, R. S. Nonsteroidal anti-inflammatory drugs and cancer prevention. *Annu. Rev. Med.* **2000**, *51*, 511−523.
(40) Sung, H.; Ferlay, J.; Siegel, R. L.; Laversanne, M.; Soerjomataram, I.; Jemal, A.; Bray, F. Global cancer statistics 2020:

https://doi.org/10.1021/acsomega.2c05746
ACS Omega 2023, 8, 3768−3784

GLOBOCAN estimates of incidence and mortality worldwide for 36 cancers in 185 countries. *Ca-Cancer J. Clin.* **2021**, *71*, 209−249.
(41) Rai, N.; Gupta, P.; Keshri, P. K.; Verma, A.; Mishra, P.; Kumar, D.; Kumar, A.; Singh, S. K.; Gautam, V. Fungal Endophytes: an Accessible Source of Bioactive Compounds with Potential Anticancer Activity. *Appl. Biochem. Biotechnol.* **2022**, *194*, 3296.
(42) Verma, A.; Gupta, P.; Rai, N.; Tiwari, R. K.; Kumar, A.; Salvi, P.; Kamble, S. C.; Singh, S. K.; Gautam, V. Assessment of biological activities of fungal endophytes derived bioactive compounds Isolated from Amoora rohituka. *J. Fungi* **2022**, *8*, 285.
(43) Ding, T.; Yang, L.-J.; Zhang, W.-D.; Shen, Y.-H. Pyoluteorin induces cell cycle arrest and apoptosis in human triple-negative breast cancer cells MDA-MB-231. *J. Pharm. Pharmacol.* **2020**, *72*, 969−978.
(44) Gotte, M.; Yip, G. W. Heparanase, hyaluronan, and CD44 in cancers: a breast carcinoma perspective. *Cancer Res.* **2006**, *66*, 10233−10237.
(45) Rai, N.; Singh, A. K.; Singh, S. K.; Gaurishankar, B.; Kamble, S. C.; Mishra, P.; Kotiya, D.; Barik, S.; Atri, N.; Gautam, V. Recent technological advancements in stem cell research for targeted therapeutics. *Drug Delivery Transl. Res.* **2020**, *10*, 1147−1169.
(46) Louderbough, J.; Schroeder, J. A. Understanding the Dual Nature of CD44 in Breast Cancer Progression. *Mol. Cancer Res.* **2011**, *9*, 1573−1586.
(47) Cho, Y.; Lee, H.-W.; Kang, H.-G.; Kim, H.-Y.; Kim, S.-J.; Chun, K.-H. Cleaved CD44 intracellular domain supports activation of stemness factors and promotes tumorigenesis of breast cancer. *Oncotarget* **2015**, *6*, 8709.
(48) Wang, X.; Decker, C. C.; Zechner, L.; Krstin, S.; Wink, M. In vitro wound healing of tumor cells: inhibition of cell migration by selected cytotoxic alkaloids. *BMC Pharmacol. Toxicol.* **2019**, *20*, 4.
(49) Khammanit, R.; Chantakru, S.; Kitiyanant, Y.; Saikhun, J. Effect of serum starvation and chemical inhibitors on cell cycle synchronization of canine dermal fibroblasts. *Theriogenology* **2008**, *70*, 27−34.
(50) Pedra, N. S.; Galdino, K. d. C. A.; da Silva, D. S.; Ramos, P. T.; Bona, N. P.; Soares, M. S. P.; Azambuja, J. H.; Canuto, K. M.; de Brito, E. S.; Ribeiro, P. R. V.; Souza, A. S. Q.; Cunico, W.; Stefanello, F. M.; Spanevello, R. M.; Braganhol, E. Endophytic fungus isolated from Achyrocline satureioides exhibits selective Antiglioma activity—the role of Sch-642305. *Front. Oncol.* **2018**, *8*, 476.
(51) Farooq, S.; Qayum, A.; Nalli, Y.; Lauro, G.; Chini, M. G.; Bifulco, G.; Chaubey, A.; Singh, S. K.; Riyaz-Ul-Hassan, S.; Ali, A. Discovery of a secalonic acid derivative from Aspergillus aculeatus, an endophyte of Rosa damascena Mill., triggers apoptosis in MDA-MB-231 triple negative breast cancer cells. *ACS Omega* **2020**, *5*, 24296−24310.
(52) Prajapati, J.; Goswami, D.; Rawal, R. M. Endophytic fungi: a treasure trove of novel anticancer compounds. *Curr. Res. Pharmacol. Drug Discov.* **2021**, *2*, 100050.
(53) Wallberg, F.; Tenev, T.; Meier, P. Analysis of apoptosis and necroptosis by fluorescence-activated cell sorting. *Cold Spring Harb. Protoc.* **2016**, *2016*, pdb.prot087387.
(54) Lee, D.; Shim, S.; Kang, K. 4, 6′-anhydrooxysporidinone from Fusarium lateritium SSF2 induces autophagic and apoptosis cell death in MCF-7 breast cancer cells. *Biomolecules* **2021**, *11*, 869.
(55) Koul, M.; Kumar, A.; Deshidi, R.; Sharma, V.; Singh, R. D.; Singh, J.; Sharma, P. R.; Shah, B. A.; Jaglan, S.; Singh, S. Cladosporol A triggers apoptosis sensitivity by ROS-mediated autophagic flux in human breast cancer cells. *BMC Cell Biol.* **2017**, *18*, 26.
(56) Kwan, Y. P.; Saito, T.; Ibrahim, D.; Al-Hassan, F. M. S.; Ein Oon, C.; Chen, Y.; Jothy, S. L.; Kanwar, J. R.; Sasidharan, S. Evaluation of the cytotoxicity, cell-cycle arrest, and apoptotic induction by Euphorbia hirta in MCF-7 breast cancer cells. *Pharm Biol.* **2016**, *54*, 1223−1236.
(57) Taritla, S.; Kumari, M.; Kamat, S.; Bhat, S. G.; Jayabaskaran, C. J. F. i. p. Optimization of PhysicoChemical Parameters for Production of Cytotoxic Secondary Metabolites and Apoptosis Induction Activities in the Culture Extract of a Marine Algal-Derived Endophytic Fungus Aspergillus sp. *Front. Pharmacol.* **2021**, *12*, 542891.
(58) Hellebrand, E. E.; Varbiro, G. Development of mitochondrial permeability transition inhibitory agents: a novel drug target. *Drug Discoveries Ther.* **2010**, *4*, 54.
(59) Tomasello, F.; Messina, A.; Lartigue, L.; Schembri, L.; Medina, C.; Reina, S.; Thoraval, D.; Crouzet, M.; Ichas, F.; De Pinto, V.; De Giorgi, F. Outer membrane VDAC1 controls permeability transition of the inner mitochondrial membrane in cellulo during stress-induced apoptosis. *Cell Res.* **2009**, *19*, 1363−1376.
(60) Alexandre, J.; Hu, Y.; Lu, W.; Pelicano, H.; Huang, P. Novel action of paclitaxel against cancer cells: bystander effect mediated by reactive oxygen species. *Cancer Res.* **2007**, *67*, 3512−3517.
(61) Chang, S.-P.; Shen, S.-C.; Lee, W.-R.; Yang, L.-L.; Chen, Y.-C. Imatinib mesylate induction of ROS-dependent apoptosis in melanoma B16F0 cells. *J. Dermatol. Sci.* **2011**, *62*, 183−191.
(62) Saleem, M. Z.; Nisar, M. A.; Alshwmi, M.; Din, S. R. U.; Gamallat, Y.; Khan, M.; Ma, T. Brevilin A inhibits STAT3 signaling and induces ROS-dependent apoptosis, mitochondrial stress and endoplasmic reticulum stress in MCF-7 breast cancer cells. *OncoTargets Ther.* **2020**, *13*, 435.
(63) Jendrossek, V. Targeting apoptosis pathways by Celecoxib in cancer. *Cancer Lett.* **2013**, *332*, 313−324.
(64) Thangam, R.; Sathuvan, M.; Poongodi, A.; Suresh, V.; Pazhanichamy, K.; Sivasubramanian, S.; Kanipandian, N.; Ganesan, N.; Rengasamy, R.; Thirumurugan, R.; Kannan, S. Activation of intrinsic apoptotic signaling pathway in cancer cells by Cymbopogon citratus polysaccharide fractions. *Carbohydr. Polym.* **2014**, *107*, 138−150.
(65) Henry, H.; Thomas, A.; Shen, Y.; White, E. Regulation of the mitochondrial checkpoint in p53-mediated apoptosis confers resistance to cell death. *Oncogene* **2002**, *21*, 748−760.
(66) Safarzadeh, E.; Sandoghchian Shotorbani, S.; Baradaran, B. Herbal medicine as inducers of apoptosis in cancer treatment. *Adv. Pharm. Bull.* **2014**, *4*, 421−427.
(67) Li, D.; Ueta, E.; Kimura, T.; Yamamoto, T.; Osaki, T. Reactive oxygen species (ROS) control the expression of Bcl-2 family proteins by regulating their phosphorylation and ubiquitination. *Cancer Sci.* **2004**, *95*, 644−650.

https://doi.org/10.1021/acsomega.2c05746
ACS Omega 2023, 8, 3768−3784